Measurement of Equivalent Input Distortion

Wolfgang Klippel

Klippel GmbH,Dresden, 01277, Germany, Fellow

ABSTRACT

A new technique for measuring nonlinear distortion in transducers is presented which considers a priori information from transducer modeling. Transducers are single input-multiple output systems (SIMO) where the dominant nonlinearities can be concentrated in a single source adding nonlinear distortion to the input signal. The equivalent input distortion at this source can easily be derived from the measured sound pressure signal by performing a filtering with the inverse transfer response prior to the spectral analysis. This technique reduces the influence of the acoustical environment (room), removes redundant information and simplifies the interpretation. It is also the basis for speeding up distortion measurements, for the prediction of distortion in the sound field and for the detection of noise and other disturbances not generated by the transducer.

1 Introduction

Traditional techniques for distortion measurements as defined in the standards determine the contamination of the output signal by spectral components which are not in the input signal but are generated by transducer nonlinearities. The results describe the nonlinear mechanisms not directly but depend on linear properties of the transducer, radiation aids, the acoustical environment (room) and sensor (microphone, laser) used. The results are usually difficult to interpret and do not reveal the physical causes. This technique is sufficient for assessing the distortion at a particular point at the diaphragm or in the sound field but less suited for describing the overall performance of the loudspeaker independent of room and sensor properties.

Thus, new ways are required for measuring distortion and post-processing to derive more meaningful information about nonlinear mechanisms in loudspeakers and the influence of the acoustical environment.

In the first part of the paper the usual way of measuring distortion is discussed and problems with the interpretation of the results are addressed. In a second part important results of loudspeaker modeling are presented which are the basis a new technique. After introducing the concept of equivalent input distortion the practical application and the relationship to the classical approach are discussed.

2 GLOSSARY OF SYMBOLS

The following symbols are used within the paper:

$Bl(x)$ nonlinear force factor depending on the voice coil displacement x

C Compression Factor in dB

$d_n^{(p)}$ nth-order harmonic distortion in the sound pressure output signal in percent (according to IEC 60268 [1])

$d_n^{(f)}$ nth-order harmonic distortion in the sound pressure output signal in percent (displayed versus measured)

$d_n^{(u)}$ equivalent nth-order harmonic distortion mapped from the sound pressure output to the input voltage in percent

$d_t^{(p)}$ total harmonic distortion in the sound pressure output in percent (according to IEC 60268)

$d_t^{(u)}$ total harmonic distortion mapped from the sound pressure output to the equivalent input voltage in percent

f frequency

f_{start} start frequency of the logarithmic sweep

f_{end} end frequency of the logarithmic sweep

$FT(f)$ Fourier transform of f

$H(f,\mathbf{r})$ linear transfer function between voltage and sound pressure at point **r**

$H_{p1}(f)$ linear pre-system connected to the first input of the static nonlinearity

$H_{p2}(f)$ linear pre-system connected to the second input of the static nonlinearity

$H_{post}(f)$ linear post-system connected to the output of the static nonlinearity

i electrical input current

$K_{ms}(x)$ stiffness of the mechanical suspension depending on the voice coil displacement

$L_e(x)$ electrical voice coil inductance depending on the voice coil displacement x

$L_n^{(p)}$ nth-order harmonic distortion in the sound pressure output signal in dB (according to IEC 60268)

$L_t^{(p)}$ total harmonic distortion in the sound pressure output signal in dB (according to IEC 60268)

n order of the harmonic distortion component

$p(\mathbf{r})$ sound pressure at point **r**

$P(f)$ spectrum of the sound pressure

P_1 fundamental component in sound pressure

P_n nth-order harmonic component in sound pressure

P_t rms-value of the total sound pressure signal

t time

T FFT length

c_0 speed of the sweep (octave per second)

u voltage at terminals

U rms voltage of the sinusoidal stimulus

U_1 equivalent fundamental component at the speaker input

U_n equivalent nth-order harmonic component mapped from the speaker output to the speaker input

v voice coil velocity

x voice coil displacement

3 HARMONIC DISTORTION MEASUREMENTS

A nonlinear system excited by a sinusoidal stimulus $u(t)=1.4U\sin(2\pi f_1 t)$ with excitation frequency f_1 will produce a distorted output signal $p(t)$ as illustrated in

Fig. 1. The spectrum $P(f)=FT\{p(t)\}$ comprises a fundamental component $P_1=P(f_1)$ and nth-order harmonic components $P_n=P(nf_1)$ with $n > 1$ located at multiples of the excitation frequency f_1.

3.1 Common Definitions

According to the IEC standard [1] the nth-order harmonic distortion may be expressed in percent

$$d_n^{(p)} = \frac{|P_n|}{P_t} 100\% \tag{1}$$

or in dB

$$L_n^{(p)} = 20\log\left(\frac{d_n^{(p)}}{100\%}\right) \tag{2}$$

using the rms-value of the total signal

$$P_t = \sqrt{\frac{1}{T}\int_0^T p(t)^2\,dt}\,. \tag{3}$$

The total harmonic distortion (THD) is the ratio between the rms value of all higher-order harmonics ($n > 1$) and the rms amplitude of the total output signal and may be expressed in percent

$$d_t^{(p)} = \frac{\sqrt{|P_2|^2 + |P_3|^2 + ... |P_n|^2}}{P_t} 100\% \ , \tag{4}$$

or in dB

$$L_t^{(p)} = 20 \log\left(\frac{d_t^{(p)}}{100\%} \right) . \tag{5}$$

3.2 Fast Measurement Technique

Many ways for the measurement of the harmonic distortion have been developed so far. Usually a sinusoidal tone has been swept continuously or stepped in increments from a starting frequency f_{start} to an end frequency f_{end}. Tracking filters with sufficient off-band rejection were used to measure the fundamental, the harmonic components or the total harmonic distortion.

Digital signal processing introduced the FFT analysis to measure the spectrum $P(f)$ directly. Setting the excitation tones at frequencies $f_k=k/T$ for any $k=1,...N$ which are synchronous with the FFT length T dispenses with windowing and separates the fundamental and harmonic components at highest spectral resolution possible. However, this technique requires a certain settling time to get the steady-state response of each tone.

Continuous sweeps require less measurement time and may give sufficient resolution in practice. The harmonics may be analyzed by performing a short-time FFT using a sliding time window. A sweep with exponential time-frequency mapping

$$f(t) = f_{start} 2^{tc_o} \quad , \tag{6}$$

with the start frequency f_{start} and the sweep speed c_0, reduces the computational work in the analysis significantly. Fig. 2 illustrate an important property of this stimulus. At time t_1 when the instantaneous frequency f_1 is supplied to the DUT the nonlinearities generate harmonics P_n with $n=2,...,N$ at the frequency nf_1. Applying the frequency-time mapping of Eq. (6) the harmonic component nf_1 corresponds with a fundamental component generated at a later time. The time difference is exactly

$$t_n - t_1 = \frac{\log_2 n}{c_o} \tag{7}$$

as long as both fundamental and harmonic components have a constant group delay.

Using this property Farina [2] suggested to separate the fundamental and higher-order harmonics in the time domain by using a deconvolution technique. A more convenient implementation is possible by using an FFT-technique as proposed by Müller [3]. Both ways lead to the time response as shown in Fig. 3. The fundamental component leads to an impulse response which is purified from all effects of higher-order harmonics. The harmonic components produce additional peaks prior to fundamental response. According to the circular property of the time response they may also be displayed at the end of the response. The temporal separation of the harmonics is a unique characteristic of the sweep. Other stimuli such as the maximal-length

sequence (MLS) applied to a nonlinear DUT generate spurious artifacts which can not be separated from the fundamental but may be easily interpreted as room reflections.

Fig. 4 shows the responses of the harmonic components in greater detail. The envelope of the harmonics decays approximately with the same time constant as the fundamental response. If the decay time is greater than

$$t_n - t_{n-1} = \frac{1}{c_o} \log_2\left(\frac{n}{n-1}\right) \tag{8}$$

the separation of nth-order and higher-order distortion is not possible anymore. This becomes a problem in the radiated sound pressure measured in the far field of the loudspeaker where the room reflections increase the length of the impulse response significantly. A solution for this problem will be presented below.

3.3 Example

The new sweep technique is very fast and provides the harmonic distortion without additional measurement time and at low computational load. For example Fig. 5 shows the fundamental component P_1, and the 2nd- and 3nd-order component P_2 and P_3 versus excitation frequency f_1 measured at 1 m distance from a vented-box system operated in a normal living room by using a sinusoidal stimulus of 10 V. The curves and all other curves presented in the following paper are smoothed with a sliding band-pass filter giving a resolution of 1/30th octave. At low excitation frequencies where the voice coil displacement is high the 3rd-order harmonic distortion exceeds the sound pressure level of the fundamental. At higher frequencies the 2nd-order harmonic distortion exceeds the 3rd-component but are 30 db below the fundamental.

Using the measured data of the example driver in Fig. 5 the relative 2nd-order harmonic distortion d_2 and the total harmonic distortion d_t are presented in Fig. 6. The total harmonic distortion varies from high values (almost 100 %) at low frequencies, where the 3rd-order component gives a significant contribution, to moderate values (about 2 %) in the pass-band where the 2nd-order harmonic d_2 dominates. Although this result is typical for harmonic distortion measurements applied to loudspeakers it should be noted that a more complex stimulus (such as a multi-tone signal or music) creates also intermodulation products in the pass-band which usually exceed the harmonic components significantly (about 20 dB).

3.4 Room Influence

The results of distortion measurements performed on loudspeakers operated under normal condition depend on the acoustical properties of the room and vary significantly with the measurement point used. For example, Fig. 7 and Fig. 8 show the 2nd- and 3rd-order harmonic distortion, respectively, measured at 1m distance and at 7 other points in a normal living room. Room modes, noise and other disturbances cause variations between 20-40 dB which dissolve most of the characteristics found in the near field measurement.

4 INTERPRETATION OF DISTORTION MEASUREMENTS

The results of distortion measurements are more difficult to interpret than the fundamental response. However, considering a nonlinear model of the loudspeaker the interpretation can be simplified and the results become much more meaningful. Clearly, modeling is basically an abstraction and can only represent essential properties of the reality.

4.1 Loudspeaker Model

Transducers which convert an electrical signal into a mechanical or acoustical signal may be modeled as a single-input and multiple-output system (SIMO). The voltage *u(t)* at the terminals is usually the input signal and the sound pressure field $p(\mathbf{r}_i)$ at any point $\mathbf{r}_i$ with *i=1, 2, ...* gives multiple outputs.

The transfer of the input signal and the distribution to the multiple outputs may be modeled by a signal flow chart as shown in Fig. 9. The signal flow between input and output may be modeled by a chain of linear and nonlinear subsystem, illustrated by thin and bold blocks, respectively. The power amplifier, passive crossover and other electronic circuits (e.g. for protection) may be considered as linear at the amplitudes used in praxis. The following electro-mechanical transducer is highly nonlinear using a moving coil in a static magnetic field and a mechanical suspension system. The voice coil displacement *x(t)* may be considered as the output of this subsystem and is also an important state variable that varies the voice coil inductance $L_e(x)$, the stiffness $K_{ms}(x)$ of the mechanical suspension and the force factor *Bl(x)*. The relationship can be described by a nonlinear differential equation [4] and can be illustrated by a signal flow chart where the displacement x at the output is fed back to the nonlinearities $L_e(x)$, $K_{ms}(x)$ and *Bl(x)*.

The mechano-acoustical transducer uses the diaphragm, the enclosure or a horn to transform the voice coil displacement into an air flow.

The air in a sealed box or the air between diaphragm and phase-plug in a horn loaded compression driver behaves nonlinearly if the variation of the air volume is not negligible.

The different modes of vibration breaking up on the diaphragm and surround at higher frequencies may also become nonlinear if the stress in the material or the deformation of the cone geometry is high.

The radiation of the sound has to be modeled by multiple subsystems which disperse the signal in different directions. For example, a driver mounted in a vented enclosure or coupled with a passive radiator has two separate sound sources. The nonlinearities of the air flow in the port or the nonlinear suspension of the passive radiator will produce distortion which is not in the sound radiated from the diaphragm of the active radiator. The partial vibrations of the cone may be radiated in a different way.

The Doppler effect depends on the radiation angle and produces phase modulation between low and high frequency components. The distortion maximum for sound radiated is in axis of the driver.

A low frequency component may also produce amplitude modulation of a high-frequency component if the cone moves with respect to the acoustical boundaries (frame, enclosure, baffle) and the radiation condition changes.

In horn compression drivers [5] the propagation of the sound wave becomes nonlinear if the sound pressure is high. A pressure maximum travels faster than a pressure minimum causing a gradual steepening of the wave front.

The interaction with the room, the superposition of the direct sound with reflected waves, may be modeled by a linear system because the air behaves sufficiently linear.

4.2 Modeling of Dominant Nonlinearities

Fortunately, most of the dominant nonlinearities which are directly related with maximum output, weight, and size of the loudspeaker and produce a high amount of signal distortion are found in the one-dimensional signal path in the electrical and mechanical system. Considering those nonlinearities only, the loudspeaker can be modeled by a simplified signal flow chart as shown in Fig. 10 . All nonlinear mechanisms in subsystems connected in series with the loudspeaker input can be concentrated in a nonlinear system generating distortion u_D which is added to the input signal u and fed back to the nonlinear system. The feedback loop causes complicated effects at high amplitudes such as compression of the output amplitude, instabilities and interactions between nonlinearities. The input signal u and nonlinear distortion u_D are transferred by a linear system $H(f,\mathbf{r})$ into the sound pressure $p(\mathbf{r})$ at point **r** in the sound field.

Consolidating nonlinearities into the single-signal path is essential for active loudspeaker linearization becoming possible with digital signal processing. If a loudspeaker can adequately be described by the model in Fig. 10 then the distortion u_D can actively be compensated by an electrical controller connected to the input of the loudspeaker. This leads to a linear transfer function between controller input and any point in the sound field. On the contrary, the equalization of the amplitude and phase response by using linear filters is always limited to a small area in the sound field. A perfect equalization of the sound pressure response at point $\mathbf{r}_1$ usually produces spectral colorations at other points in the sound field.

Most of the dominant nonlinear mechanisms found in loudspeakers can be described by models which are based on the Multi Memory Decomposition (MMD) technique [6] as shown in Fig. 11.

Each MMD system models the effect of a particular nonlinearity. It comprises linear pre-systems H_{p1} and H_{p2}, a static nonlinearity which multiplies the output of H_{p1} and H_{p2} by using a nonlinear parameter, and a linear post-system H_{post}. The multiplication of time signals is the critical operation which generates the harmonic and other intermodulation components. The linear post-system $H_{post}(f)$ connected to the output of the static nonlinearity finally shapes the amplitude and phase of the generated distortion. Table 1 specifies the elements of the MMD model for the dominant nonlinear mechanisms in electro-dynamic loudspeakers. The linear pre- and post-systems determine the spectral properties of the distortion. The pre-system has a major influence on the generation of the distortion. Clearly the nonlinear suspension of a woofer mainly produces distortion at low frequencies because a low-pass filtered signal (voice coil displacement) is multiplied with itself. Usually a variation of the amplitude response in the pre-system causes a variation of squared, cubic or higher power in the output distortion. The post-system shapes the distortion product linearly. For example a differentiator enhances all distortion products caused by the nonlinear inductance $L_e(x)$ in the input impedance by 6 dB per octave.

The static nonlinearity mainly determines the relationship between input signal and amplitude of a distortion component at the output. For example, comparing two drivers using the same coil but different gap heights, the driver with the larger voice coil overhang gives much less distortion at small and medium amplitudes but the distortion suddenly rises if the coil leaves the gap approaching to the same distortion at high amplitudes as the driver with small voice coil overhang.

4.3 Graphical Representation

The graphical presentation of the distortion component is crucial for the interpretation of the distortion measurements. Historically, the absolute and the relative amplitude of the harmonic distortion components have been plotted versus the excitation frequency, which is identical with the fundamental component. This is widely used and has become an international standard.

Alternatively, the distortion components may be also plotted versus their actual frequency as found in the analyzed spectrum.

The benefits and drawbacks of both ways are discussed for a simple example using the idealized amplitude responses of the pre-system and post-system given in Fig. 12.

A low-pass characteristic is used for the pre-systems H_{p1} and H_{p2} to describe the displacement of the voice coil. A notch at the tuning frequency f_1 is caused by the acoustical resonance of the vented enclosure. Above the driver's resonance f_S the amplitude decays with a slope of 12 dB/octave. Since the post-system H_{post} has also a constant amplitude response the nonlinear subsystem may describe a nonlinear suspension. The linear system $H(f)$ between input voltage and sound pressure output at point **r** has a typical high-pass characteristic above the frequency f_1. The narrow peak at frequency f_2 is caused by an acoustical room resonance.

4.3.1 Display versus excitation frequency

According to the international standard the fundamental P_1 and the higher order harmonic components P_2, P_3 are plotted in

Fig. 13 versus the excitation frequency. The amplitude response of harmonics is a combination of the pre-system, the post-system and the linear system $H(f)$. The dip in the pre-system H_{p1} and

H_{p2} at tuning frequency f_1 and the slope above the driver resonance f_S reduces the distortion components P_2, P_3 at the same frequencies. However, the size of the dip and the steepness of the slope rise with the order n of the measured harmonic P_n.

The amplitude response of post-system H_{post} and the linear response $H(f,\mathbf{r})$ shapes the output spectrum linearly. Displaying the nth order harmonics versus excitation frequency, however, shows the room resonance and the slope of the high-pass characteristic of the linear response at nth part of the excitation frequency.

Calculating the relative distortion d_2 and d_3 according to Eq, (1) shows the percentage of distortion in output signal as shown for the idealized speaker in

Fig. 14. The relative distortion rises either for a higher amplitude of the nonlinear component or for a lower amplitude of the fundamental component. Here the curves become even more complex and it is really difficult to understand the nonlinear mechanism and to identify the relatively simple responses $H_{p1,}$ H_{post} and H.

However, the traditional way of displaying harmonic distortion is useful to evaluate the overall system which includes the loudspeaker and the influence of the acoustical environment and may vary significantly with the listening position.

4.3.2 Display versus measured frequency

Alternatively, the distortion component and linear signal may be plotted versus measured frequency as shown in Fig. 15.

Here the spectral features of the post-system H_{post} and the linear response *H(f)* appear at the same frequencies. Consequently, the notch and the slope of the high-pass of the pre-system are shifted to *n* times the fundamental frequency.

Calculating a relative value for each nth-order harmonic distortion

$$d_n{}^f(f) = \frac{|P_n(f/n)|}{|P_1(f)|} 100\% \tag{9}$$

as the amplitude ratio of the nth-order component generated by the excitation frequency f/n referred to the amplitude of the fundamental component at frequency *f*. The superscript *f* in d_n^f indicates the mapping to the measured frequency to distinguish it from the standard defined in Eq, (1). In this measure the effect of the amplitude response *H(f)* is removed and the harmonic distortion reveals only the effect of the nonlinear subsystem. For example, the peak caused by the room resonance and the high-pass characteristic of the loudspeaker does not appear in

Fig. 16. Thus, the relative distortion according to Eq. (9) shows more clearly the generation of the *n*th-order distortion component and suppresses the influence of linear transfer path (radiation, room).

Unfortunately, this approach has some major disadvantages. First, the display versus measured frequency corresponds neither with the current standard nor the usual way of measuring distortion. This may cause some confusion in practical handling. Second, the frequency responses of the distortion components in Eq. (9) are also difficult to interpret. Features of the amplitude response H_{pl} such as the notch and the slope in Fig. 12 appear at *n*-times the original frequency in

Fig. 16 depending on the order n of the distortion component. Third, it makes no sense to sum up all nth-order distortion (for $n > 1$) to calculate the total harmonic distortion because the distortion components displayed versus measured frequency are generated by different fundamentals.

5 EQUIVALENT INPUT DISTORTION

The signal U_D at the output of the nonlinear system as shown in Fig. 10 describes the distortion directly at the source of the dominant loudspeaker nonlinearities. Since a direct measurement at this point is not possible, the distortion U_D have to be calculated from the output signal $p(r)$ measured at point **r** in the sound field. This can be accomplished by a simple filtering of the measured sound pressure $p(t)$ with the inverse system function $H(f,\mathbf{r})^{-1}$ as illustrated in Fig. 17.

Performing an FFT of the filtered output $u(t)+u_D(t)$ the spectral components

$$U_n = \frac{P_n}{H(nf)} = \frac{P(nf)}{H(nf)} \tag{10}$$

for $n>0$ are calculated. U_1 is the equivalent input fundamental which reflects the amplitude of the input stimulus $u(t)$ and the nonlinear distortion component at the fundamental frequency. At sufficiently small amplitude the fundamental U_1 equals the input stimulus U. At higher amplitudes the loudspeaker's nonlinearities cause a compression of the fundamental's amplitude $U_1 < U$ which may be described by a compression factor

$$C = -20\log\left(\frac{|U_1(f)|}{|U(f)|}\right). \tag{11}$$

in dB.

The harmonics U_n for $n>1$ are the equivalent input harmonics at the electrical terminals of the "linearized" loudspeaker.

The linear transfer function $H(f)$ required in Eq. (10) is defined by

$$H(f) = \frac{P_1(f)}{U_1(f)} \tag{12}$$

using the fundamental $P_1(f)$ and the distorted fundamental component U_1 .

For $u >> u_D$ the transfer function can be approximated by

$$H(f) \approx \frac{P_1(f)}{U(f)} . \tag{13}$$

using the amplitude $U(f)$ of the undistorted stimulus. The condition can always be realized since u_D is a nonlinear function of u and vanishes for sufficiently small input amplitude U. If necessary an additional measurement with reduced input voltage U has to be performed.

For example Fig. 18 shows the equivalent fundamental input and the harmonic distortion components of 2nd- and 3rd-order for the speaker having the idealized responses in Fig. 12.

The amplitude of the fundamental component U_1 is almost constant because the nonlinear compression is usually small. The 2nd-order component U_2 and the 3rd-order component U_3 reveals the notch and the slope at the same tuning frequency f_1 and the cut-off frequency f_2 as the pre-system H_{p1} and H_{p2}. Clearly the amplitude variations increase with the order of the component.

In an analogue way as in the IEC standard the relative nth-order equivalent input distortion

$$d_n^{(u)} = \frac{|U_n|}{U_t} 100\% \tag{14}$$

for $n > 1$ is defined as the ratio of the amplitude of the nth-order harmonic component referred to the rms value of the total voltage signal

$$U_t = \sqrt{\frac{1}{T}\int u(t)^2 + u_D(t)^2 dt} \,. \tag{15}$$

For $u >> u_D$ the nth-order equivalent input distortion according to Eq. (14) becomes identical with the relative distortion suggested by Temme [7] using amplitude normalization according Eq. (9) and additional frequency shifting to the excitation frequency.

Using the data of the real loudspeaker used in Fig. 5 the equivalent input components U_1, U_2 and U_3 are presented in Fig. 20. Below 40 Hz there is a compression of the fundamental component U_1 but at higher frequencies U_1 is close to the input voltage U=10 V rms. The 3rd-order component U_3 of the equivalent input distortion exceeds 2 V rms below 40 Hz but stays below 200 mV rms at higher frequencies. The 2nd-order input distortion is only half the value of the 3rd-order component below 50 Hz but becomes dominant at higher frequencies.

Fig. 21 and Fig. 22 show the relative 2nd- and 3rd-order distortion $d_n^{(u)}$ in percent according to Eq. (14) as thick lines. Since the amplitude U_1 of the fundamental component is almost constant versus frequency the relative distortion curves have almost the same shape as the corresponding absolute distortion components in Fig. 20.

As for Eq. (4), all higher-order distortion can be summed up to the total harmonic distortion

$$d_t^u = \frac{\sqrt{|U_2|^2 + |U_3|^2 + ... |U_3|^2}}{U_t} 100\% \tag{16}$$

equivalent at the input. The total harmonic distortion d_t^u can directly be compared with the *n*th-order equivalent distortion d_n^u because both curves refer to the same excitation frequency *f*. The total equivalent harmonic distortion displayed in Fig. 23 is dominated below 50 Hz by the 3rd-order distortion $d_3^{(u)}$ and at higher frequencies by the 2nd-order distortion $d_2^{(u)}$.

Fig. 21 - Fig. 23 also show the equivalent input distortion measured at 0.1 and 0.5 m distance as thin lines. The results match very well the corresponding distortion measured at 1 m distance (thick line). However, between 1 and 3 kHz there are significant differences. The partial vibrations breaking up at particular frequencies become nonlinear and produce distortion products which are not radiated in the same way as the fundamental component. For these frequencies the nonlinearities are not restricted to the one-dimensional domain but are distributed over the multi-dimensional signal paths leading to different points in the sound field. In this case multiple measurement performed in the sound field do not result in the same equivalent distortion at the input.

5.1 Separating Loudspeaker and Room

The calculation of the equivalent input distortion is a convenient way to assess the nonlinear properties of a loudspeaker operated in a room and to remove the influence of the room modes. This is for example required if the performance of an automotive loudspeaker has to be investigated on the basis of sound pressure measurements taken at the passenger's ears in a car. The same technique may also be used in larger rooms to check a sound reproduction system. For example the 2nd-order and 3rd-order distortion in the sound pressure measured at 1 m and 8 other

points in a living room as presented in Fig. 7 and Fig. 8 are transformed into the equivalent distortion and presented in Fig. 24 and Fig. 25. The variation of the curves is substantially reduced and the fine structure of the distortion response becomes visible and agrees with the curve measured at 1 m distance (thick line). It is also typical that most of the equivalent distortion curves measured in the far field are above the equivalent distortion derived from near-field measurements. This is mainly caused by residual noise and other stationary or transient disturbances corrupting the distortion measurement as discussed in detail below.

5.2 Speeding up measurement

The concept of measuring equivalent distortion makes it also possible to measure higher-order harmonics in rooms causing a long decay time of the impulse response. As outlined in section 3.2, two higher-order responses can only be separated in the time domain if the response of the nth-order harmonic is sufficiently decayed before the *(n-1)*th-order response arrives. Since the calculation of equivalent distortion is basically an equalization of the linear transfer response prior to the spectral analysis, the decay process both of the fundamental and the harmonics will be significantly faster as shown in Fig. 26 compared with the original time response given in Fig. 3. The fundamental response is almost a direct impulse while the higher-order harmonics shown in Fig. 27 can also be separated more easily.

5.3 Practical Usage

The following procedure is recommended to measure the equivalent fundamental response and distortion:

1. Set the microphone in the near field of the loudspeaker where the signal to noise ratio in the measured sound pressure is sufficient to measure harmonic distortion.

2. Measure the sound pressure signal at high and low amplitudes by using the fast sweep technique.

3. Equalize the sound pressure signal measured at high amplitude by using the inverse linear transfer function $H(f,\mathbf{r})^{-1}$ measured at low amplitude.

4. Analyze the fundamental and the harmonic components.

5. Present the components in volts or calculate the relative distortion in percent.

6 PREDICTION OF HARMONIC DISTORTION

The measurement of the equivalent distortion provides the fundamental U_1 and the harmonic components U_2, U_3 , ... equivalent to the input of a "linearized" loudspeaker. These curves may be measured at one point in the near field where the influence of noise and other disturbances is small. Based on this information it is possible to predict the fundamental and the harmonic distortion components

$$P_n(\mathbf{r}) = H(nf, \mathbf{r})U_n \tag{17}$$

at any point in the sound field by applying a linear filtering with the transfer function $H(f,\mathbf{r})$ to the equivalent distortion as illustrated in Fig. 28.

For example, multiplication of the linear transfer function $H(f,\mathbf{r}_7)$ measured at small amplitudes between loudspeaker terminals and point $\mathbf{r}_7$ with the equivalent fundamental response U_1, the equivalent input distortion U_2 and U_3 given in Fig. 20, leads to the fundamental P_1, 2nd-order distortion P_2 and 3rd-order harmonic distortion P_3 given in Fig. 29 and Fig. 30, respectively.

Using the same fundamental U_1 and harmonic distortion responses U_2 and U_3 equivalent in the input voltage but combining it with a different linear transfer function $H(f,\mathbf{r}_5)$ leads to the sound pressure responses at a different point $\mathbf{r}_5$ in the sound field as presented in Fig. 31 and Fig. 32. All these predictions match the direct measurements performed at the same point with sufficient accuracy. The minor deviations have the following causes:

- Nonlinearities in the multi-dimensional signal path which are not perfectly described by the equivalent input distortion.
- Noise and other disturbances generated by external sources may corrupt the distortion measurement performed in the far field of the loudspeaker.

7 SEPARATION OF NOISE AND DISTURBANCES

Noise and disturbances from sound sources other than the loudspeaker can easily corrupt a distortion measurement because the sound pressure level of the harmonics is usually very small. Loudspeaker are also used in applications where the enclosure, the radiation aid or other parts are not rigid enough and perform nonlinear vibrations excited by the loudspeaker signal. Typical examples are injection molded enclosures used for inexpensive audio equipment but also automotive applications where the loudspeaker is mounted in a door or hat rest. The additional disturbances found in the sound pressure signal can be separated from loudspeaker distortion by comparing the results of a distortion measurement with the results of the prediction based on equivalent distortion.

The following procedure is recommended:

1. Measure the equivalent distortion in the near field of the loudspeaker according to section 5.3 where the radiated sound pressure is high in comparison to noise and other disturbances.

2. Measure the linear transfer response $H(f,\mathbf{r})$ between loudspeaker input and any point r in the sound field.

3. Multiply the frequency response $H(f,\mathbf{r})$ with the equivalent fundamental and the equivalent input distortion according to Eq. (17).

4. Measure the harmonic distortion in the radiated sound field at point **r** at high amplitudes.

5. Compare the measured and predicted distortion components in volts or as relative distortion in percent.

Noise and the different kinds of disturbances cause characteristic disagreements between the measured and predicted distortion if a logarithmic sweep is used as stimulus.

7.1 Stationary Disturbances

If the measured sound pressure signal is corrupted by a tone at frequency f_c which is stationary during the sweep measurement then the disturbance appears in the nth-order harmonic components P_n at frequencies f_c/n. For example, a fan generating a tonal disturbance with a distinct component at about 1 kHz will disturb the 2nd-order harmonic distortion at 500 Hz and the 3rd-order distortion at 330 Hz. This can be easily detected in Fig. 33 and Fig. 34 by comparing the measured and predicted responses.

7.2 Transient Disturbances

A transient disturbance that occurs during a sweep measurement increases all harmonics at the same excitation frequency which directly corresponds with the time when the disturbances corrupted the sound pressure signal. For example, shutting the door produced in 2^{nd}-and 3^{rd}-order harmonics in Fig. 35 and Fig. 36, respectively, almost the same disturbance between 1000 – 1500 Hz. This can be easily detected by comparing the measured response with the predicted response. A parasitic vibration initiated at a certain excitation frequency has a similar characteristic.

7.3 Noise

Broad-band noise generated by external sources or within the measurement system (microphone, amplifier, AD converter) usually fills up the dips in the frequency response of the higher-order hamonics. For example, Fig. 37 shows the predicted and measured 5^{th}-order harmonic distortion measured at a remote point in the room. The thick line represents the distortion predicted from the equivalent harmonics measured in the near field of the loudspeaker. The 5^{th}-order component measured at the remote point exceeds the predicted response by more than 20 dB above 500 Hz and can easily be identified as noise.

8 CONCLUSIONS

Because the loudspeaker may be considered as a single-input but multiple output system (SIMO), multiple measurements of distortion in the sound field produce a large amount of data which are difficult to interpret. However, a major part of this information is redundant with the linear transfer response $H(f,\mathbf{r})$ measured between loudspeaker input and any point **r** in the sound

field at small amplitudes. The new concept of equivalent input distortion as presented in this paper separates the essential nonlinear information from the linear information.

This measurement technique is closely related with loudspeaker modeling, because most of the dominant nonlinearities are located in the electrical and mechanical part and can be concentrated in a distortion source adding distortion to the loudspeaker input. If the following signal path to any point in the sound field is sufficiently linear then there is a direct relationship between the distortion measured in the sound field and the equivalent input distortion. Using a linear filter with the inverse linear transfer response of the loudspeaker, this path can be equalized and the equivalent input distortion derived from the measured sound pressure distortion and vice versa. This technique has been applied to harmonic distortion in this paper but it is also useful for any kind of distortion measurement (e.g. intermodulation). In both cases the amount of measurement data can be substantially reduced and more easily interpreted. A loudspeaker may be described by two sets of data: The linear set comprises an amplitude and phase response $H(f,\mathbf{r})$ for each point **r** in the sound field. The nonlinear set comprises for each order n of the equivalent input distortion only one frequency response U_n (with $n \geq 1$). Thus, the equivalent input distortion describes the large signal performance of the loudspeaker without room influence.

The linear frequency response of the sensor used for the measurement of the loudspeaker output has no influence on the calculated equivalent input distortion. Thus, a precise or inexpensive microphone or even a laser measuring displacement, velocity or acceleration of the cone will result in the same equivalent distortion as long as the sensor behaves linearly, there is sufficient signal to noise ratio and the loudspeaker nonlinearities are only located in the one-dimensional signal path.

The equivalent fundamental U_1 compared with the input voltage U reveals the nonlinear compression.

The equalization of the measured sound pressure signal prior to the spectral analysis speeds up the measurement of harmonic distortion in rooms using fast sweeps because the higher-order harmonics can still be separated in the time domain.

The distortion may be predicted at any point **r** in the sound field by a simple multiplication of the equivalent distortion with the linear transfer response $H(f,\mathbf{r})$ according Eq. (17). This technique might be useful for the installation and adjustment of loudspeakers used in public address applications.

The comparison of predicted and measured distortion reveals noise and disturbances caused by parasitic vibrations (enclosure, door) which can be separated from loudspeaker distortion.

The equivalent input distortion helps to identify the properties of the pre-systems H_{p1}, H_{p2} and the post-system H_{post} of the MMD-model in Fig. 11. Excessive equivalent distortion $U_n(f)$ occurring as distinct peaks at the same frequency f for different orders n indicate a peak in the frequency response of the pre-systems H_{p1} and H_{p2} which can be reduced by an electrical filter connected to the input of the loudspeaker. For the same reason a high-pass with a cut-off frequency close to the tuning frequency reduces the distortion of a vented-box system in a most efficient way. If excessive equivalent input distortion U_n is found at distinct frequencies nf shifted by the order n then peaks in the frequency response H_{post} of the post-system have to be removed by coping with partial vibrations on the diaphragm or acoustical resonances.

If the equivalent distortion curves derived from sound pressure measurements at different locations (at sufficient signal to noise ratio) does not agree then the deviation reveal dominant

nonlinearities in the multi-dimensional signal path which can not be mapped to the same equivalent input distortion in the one-dimensional path. Thus, nonlinearities in the partial vibration, radiation and acoustical system can be recognized and distinguished from motor and suspension nonlinearities.

Driving loudspeakers with a current source or any amplifier with high output impedance the equivalent distortion may be calculated in the input current or mapped into the signal at amplifier input. Thus, the concept of equivalent distortion is very convenient to assess the large signal performance of active loudspeaker systems.

Finally, the measurement of equivalent input distortion is crucial for the development of nonlinear control structures dedicated to loudspeakers. The equivalent input distortion describes the required compensation signal synthesized by an electrical controller in Fig. 38. Only the loudspeaker nonlinearities located in the one-dimensional signal path can be completely compensated by active linearization.

9 REFERENCES

[1] “Sound System Equipment. Part 5: Loudspeakers,” IEC Publication 60268-5

[2] A. Farina, “Simultaneous Measurement of Impulse Response and Distortion with a Swept-Sine Technique,” presented at the 108th Convention of the Audio Engineering Society, J. Audio Eng. Soc. (Abstracts), vol. 48, p. 350 (2000 Apr.), preprint 5093.

[3] S. Müller, P. Massarani, “Transfer-Function Measurement with Sweeps,” J. Audio Eng. Soc. 20001, June, Vol. 49, No. 6, pp. 443-471.

[4] A. J. Kaiser, “Modeling of the Nonlinear Response of an Electrodynamic Loudspeaker by a Volterra Series Expansion,” J. Audio Eng. Soc. 35, p. 421, (1987 Juni).

[5] W. Klippel, “Modeling the Nonlinearities in Horn Loudspeakers,” J. Audio Eng. Soc., vol. 44, pp. 470-480 (1996).

[6] W. Frank, “MMD - An Efficient Approximation to the 2nd Order Volterra Filter,” Proc. Int. Conference of Acoustics, Speech and Signal Processing, Adelaide, Australia, pp. III 517-520, April 1994.

[7] S. F. Temme, “How to Graph Distortion Measurements, ” presented at the 94th Convention of Audio Eng. Soc. , 1993 March 16-19, Berlin, preprint 3602.

[8] “Measurement of Equivalent Input Distortion,” Application Note AN 20 of the Klippel Analyzer System, www.klippel.de.

Captions of the Figures:

Fig. 1: Measurement of harmonic distortion in the spectrum *P(f)* of the output signal

Fig. 2: Fast measurement of fundamental and harmonic components by using a logarithmic sweep as stimulus

Fig. 3: Separation of the fundamental response (left) and harmonic responses (right) in the time domain.

Fig. 4: Detail of the time response representing the 2nd-, 3rd- and higher-order harmonics in the sound pressure at the point r in the sound field (loudspeaker + room)

Fig. 5: Amplitude response of fundamental component *P1* (dashed line), 2nd-order harmonic component *P2* (thin line) and 3rd-order harmonic component *P3* (thick line) versus excitation frequency.

Fig. 6: Amplitude response of 2nd-order harmonic distortion *d2* (solid line) and of total harmonic distortion *dt* (thin line) in percent of the total signal component versus excitation frequency.

Fig. 7: 2nd-order harmonic distortion in percent measured at 1m distance (thick line) and at 7 other microphone positions in a room (thin lines).

Fig. 8: 3rd-order harmonic distortion in percent measured at 1m distance (thick line) and at 7 other microphone positions in a room (thin lines).

Fig. 9: Signal flow chart

Fig. 10: Loudspeaker modeling considering the dominant nonlinearities

Fig. 11: Modeling of nonlinear mechanism by a MMD systems.

Fig. 12: Amplitude responses (at low frequencies) of the linear pre-system *Hpre* and the linear transfer function *H(f)* of an idealized loudspeaker

Fig. 13: Amplitude response of the fundamental component *P1,* the 2nd-order component *P2* and the 3rd-order component *P3* displayed versus **excitation** frequency *f.*

Fig. 14: Amplitude response of 2nd-order distortion *d2* and 3rd-order distortion *d3* in percent displayed versus **excitation** frequency *f.*

Fig. 15: Amplitude response of the fundamental component *P1,* the 2nd-order component *P2* and the 3rd-order component *P3* displayed versus **measured** frequency *f, 2f, 3f,* respectively .

Fig. 16: Amplitude response of 2nd-order distortion *d2* and 3rd-order distortion *d3* in percent displayed versus **measured** frequency *2f, 3f,* respectively .

Fig. 17: Measurement of equivalent input distortion by performing a inverse filtering prior to the signal analysis

Fig. 18: Fundamental component *U1* and equivalent 2nd-order and 3rd-order harmonic distortion, *U2* and *U3,* respectively, mapped to the electrical voltage at the loudspeaker input displayed versus excitation frequency *f.*

Fig. 19: Amplitude response of 2nd-order distortion *d2* and 3rd-order distortion *d3* in percent displayed versus excitation frequency f .

Fig. 20: Equivalent input fundamental *U1* (upper line), 2nd-order equivalent input distortion *U2* (thin line) and 3rd-order equivalent input distortion (thick line) in Volt derived from sound pressure measurement at 1 m distance.

Fig. 21: 2nd-order harmonic distortion equivalent at the input derived from sound pressure measurement at 0.1 m, 0.5 m (thin lines) and 1 m distance (thick line).

Fig. 22: 3rd-order harmonic distortion equivalent at the input derived from sound pressure measurement at 0.1 m, 0.5 m (thin lines) and 1m distance (thick line).

Fig. 23: Total harmonic distortion equivalent at the input derived from sound pressure measurement at 0.1 m, 0.5 m (thin lines) and 1 m distance (thick line).

Fig. 24: Equivalent 2nd-order harmonic distortion in percent measured at 1m distance and at 8 different microphone positions in a normal living room.

Fig. 25: Equivalent 3rd-order harmonic distortion in percent measured at 1m distance and at 8 different microphone positions in a normal living room.

Fig. 26: Time Response of the pre-filtered sound pressure signal.

Fig. 27: Detail of the time response in Fig. 26 representing the 2nd-order and 3rd-order equivalent harmonics.

Fig. 28: Prediction of the fundamental and harmonics in the sound pressure output based on equivalent harmonic distortion filtered with the linear transfer function *H(f,r)*.

Fig. 29: Fundamental response *P1* and 2nd-order harmonic distortion component *P2* measured and predicted at point **r7** in the room.

Fig. 30: Fundamental response *P1* and 3rd-order harmonic distortion component *P3* measured and predicted at point **r7** in the room.

Fig. 31: Fundamental response *P1* and 2nd-order harmonic distortion component *P2* measured and predicted at point **r5** in the room.

Fig. 32: Fundamental response *P1* and 3rd-order harmonic distortion component *P3* measured and predicted at point **r5** in the room.

Fig. 33: Detection of a stationary disturbance (1 kHz tone) in the 2nd-order harmonic distortion component by comparing the predicted and measured distortion.

Fig. 34: Detection of a stationary disturbances (1 kHz tone) in the 3rd-order harmonic distortion component by comparing the predicted and measured distortion.

Fig. 35: Separation of a transient disturbance (shutting the door) by comparing the predicted and measured 2nd-order harmonic distortion component *P2*.

Fig. 36: Separation of a transient disturbance (shutting the door) by comparing the predicted and measured 2nd-order harmonic distortion component *P2*.

Fig. 37: Detection of a disturbances (noise) in the 5th- harmonic distortion component by comparing the predicted (thick line) and measured (thin line) distortion.

Fig. 38: Active Compensation of Equivalent Input Distortion by Nonlinear Control.

Caption of the Table:

Table 1: Properties of the linear systems and the static nonlinearity

FIGURES:

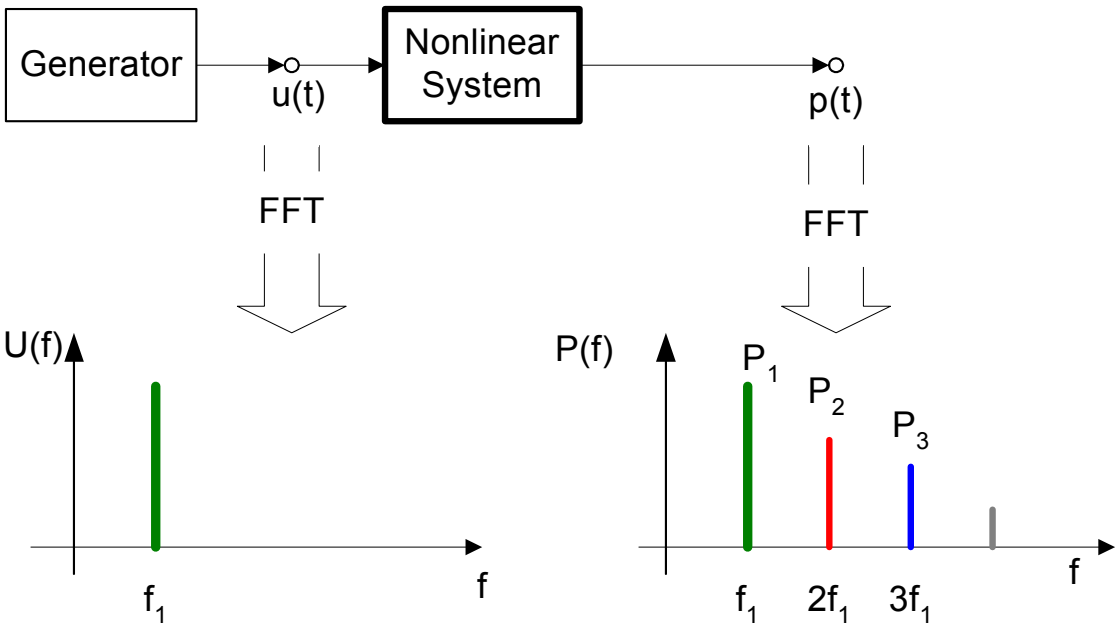

Fig. 1: Measurement of harmonic distortion in the spectrum *P(f)* of the output signal

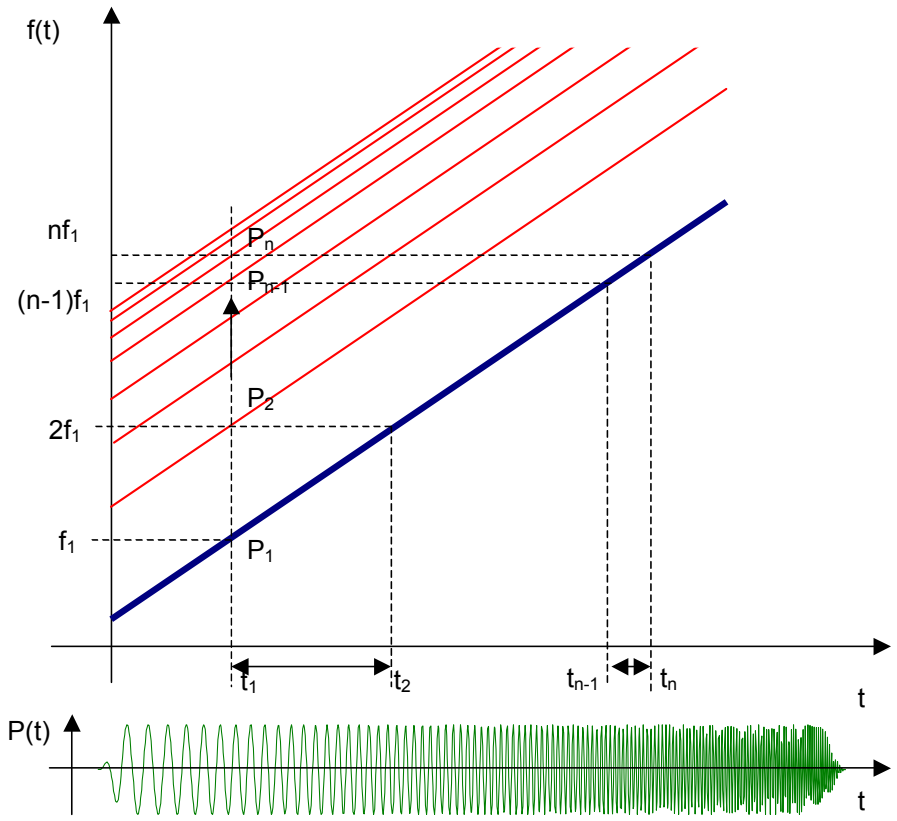

Fig. 2: Fast measurement of fundamental and harmonic components by using a logarithmic sweep as stimulus

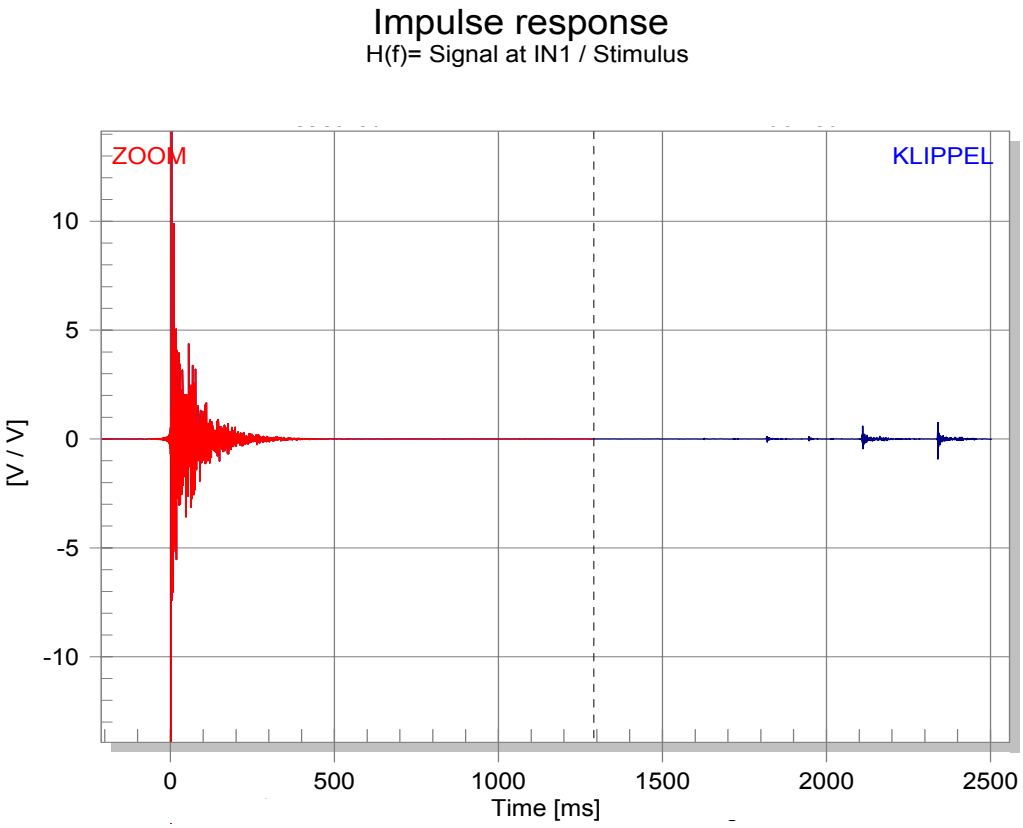

Fig. 3: Separation of the fundamental response (left) and harmonic responses (right) in the time domain.

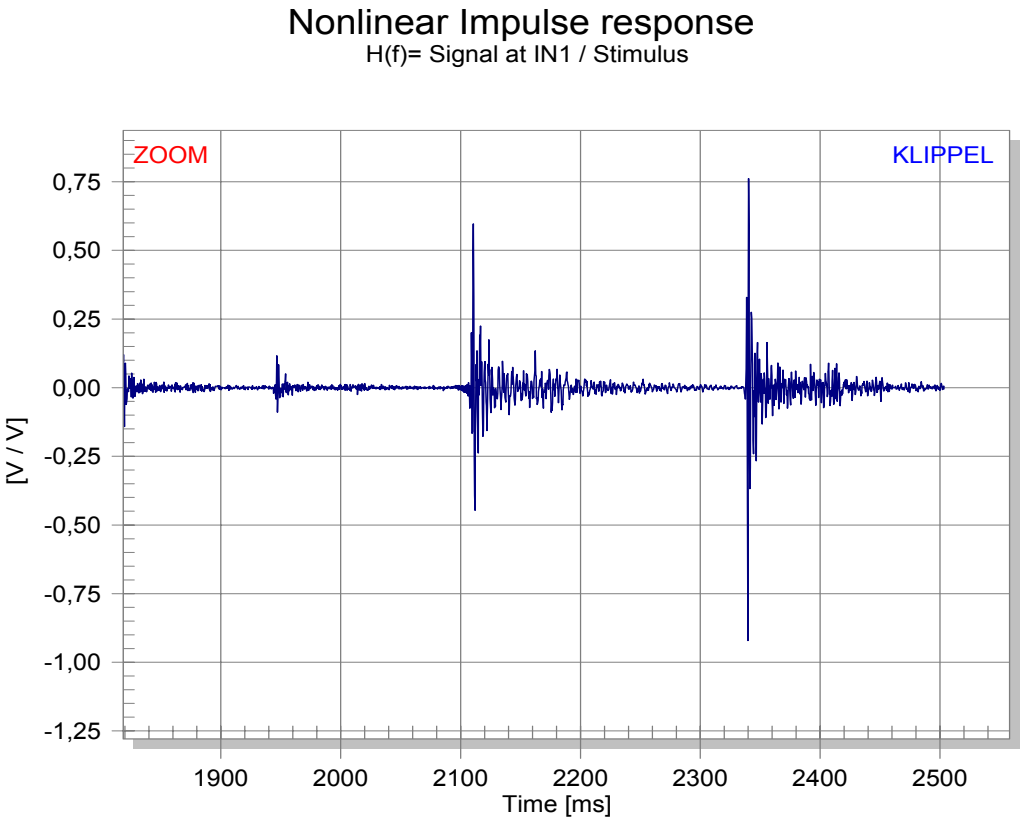

Fig. 4: Detail of the time response representing the 2nd-, 3rd- and higher-order harmonics in the sound pressure at the point r in the sound field (loudspeaker + room)

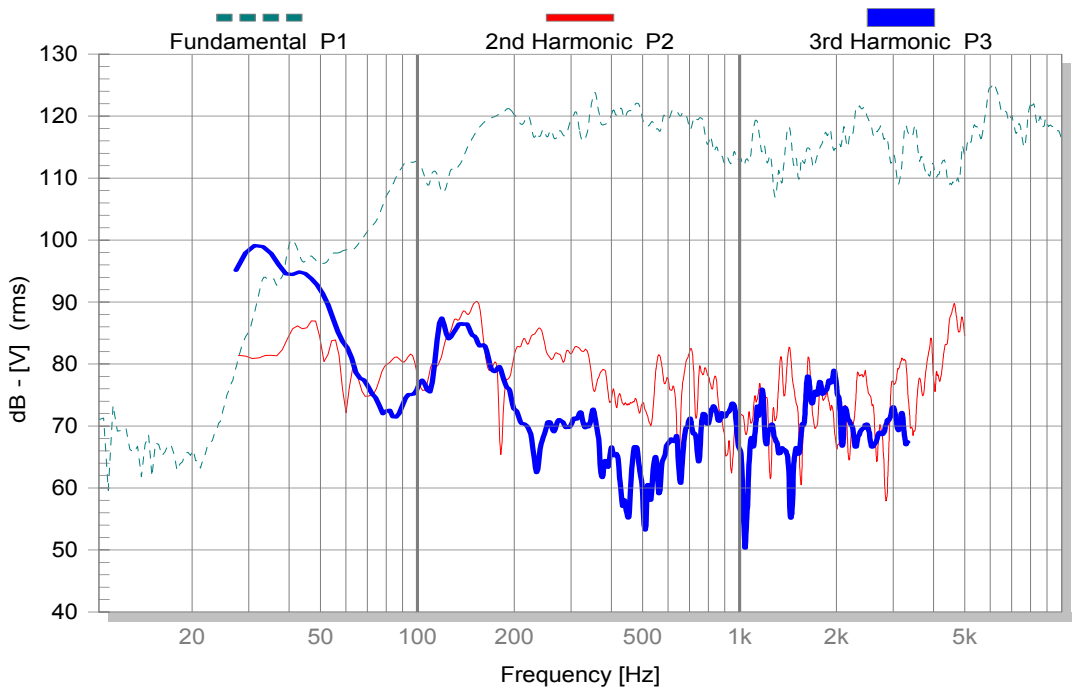

Fig. 5: Amplitude response of fundamental component P_1 (dashed line), 2nd-order harmonic component P_2 (thin line) and 3rd-order harmonic component P_3 (thick line) versus excitation frequency.

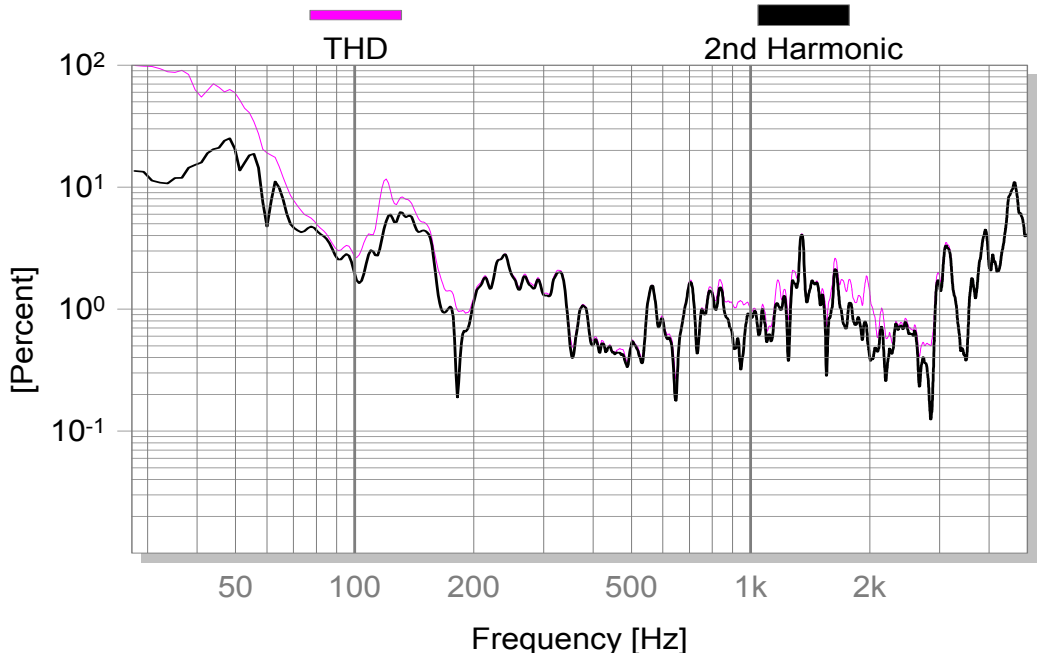

Fig. 6: Amplitude response of 2nd-order harmonic distortion d_2 (solid line) and of total harmonic distortion d_t (thin line) in percent of the total signal component versus excitation frequency.

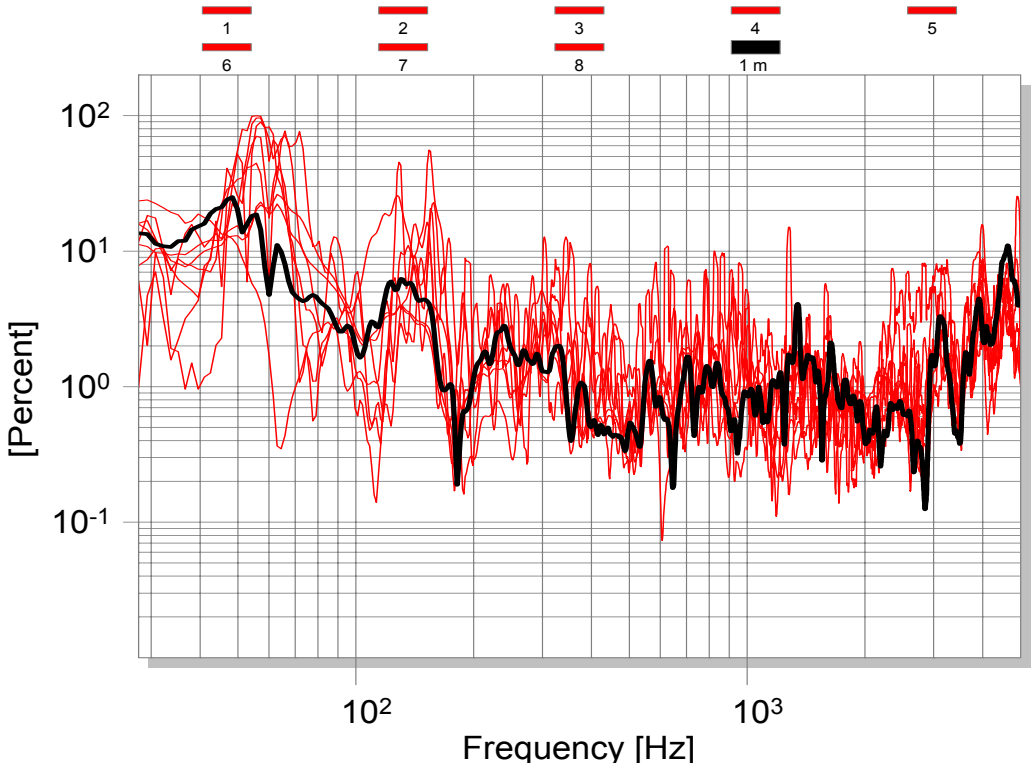

Fig. 7: 2nd-order harmonic distortion in percent measured at 1m distance (thick line) and at 7 other microphone positions in a room (thin lines).

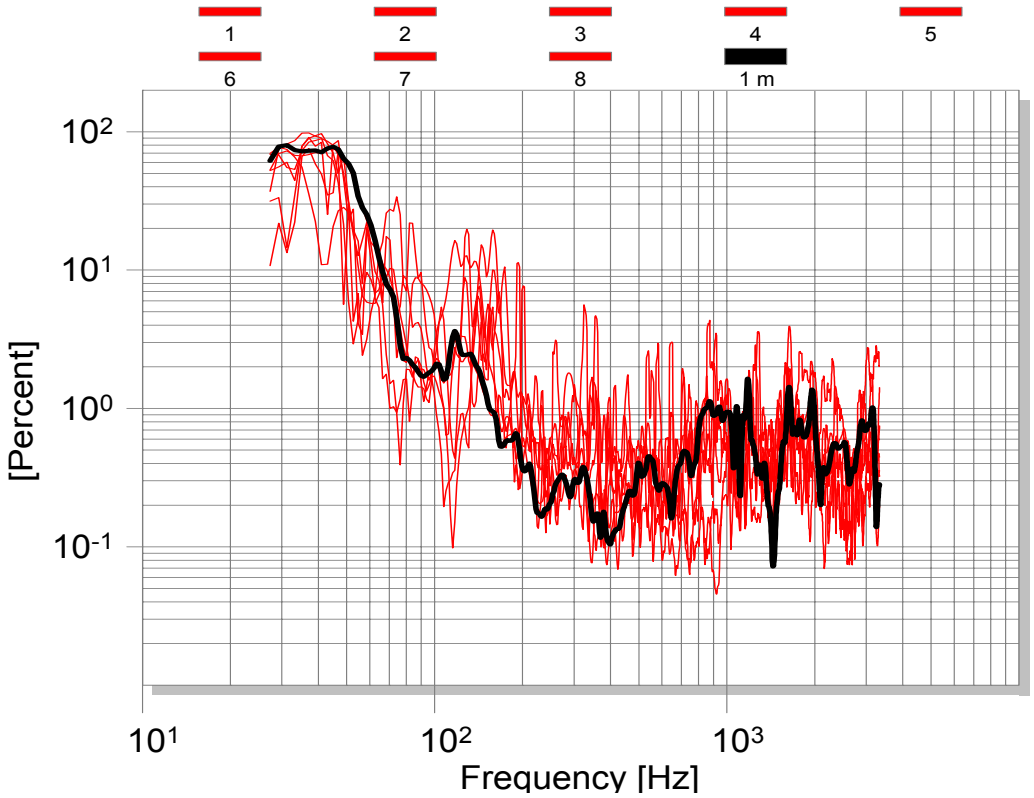

Fig. 8: 3rd-order harmonic distortion in percent measured at 1m distance (thick line) and at 7 other microphone positions in a room (thin lines).

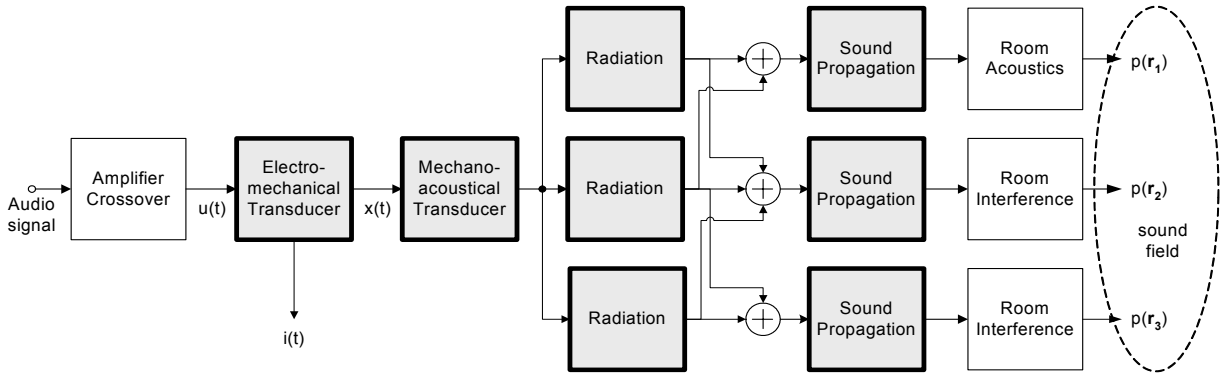

Fig. 9: Signal flow chart

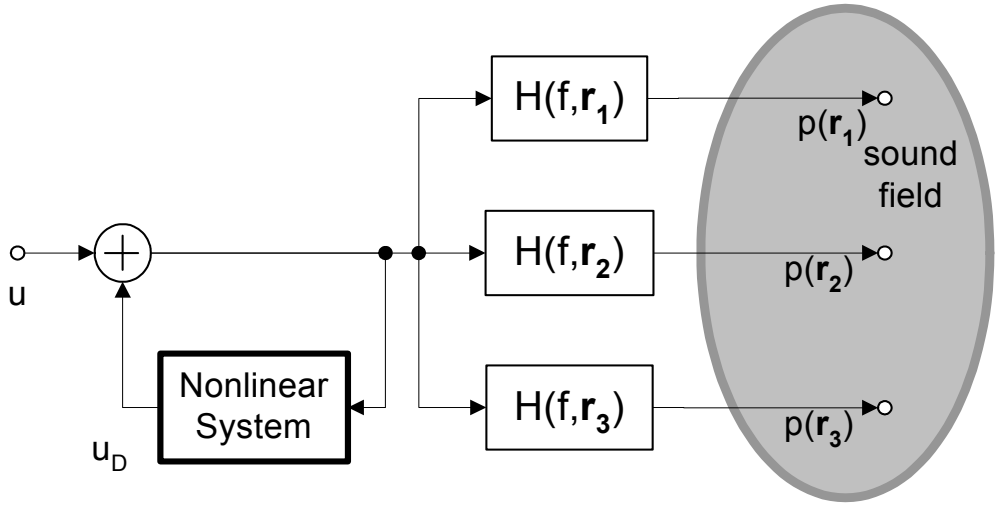

Fig. 10: Loudspeaker modeling considering the dominant nonlinearities

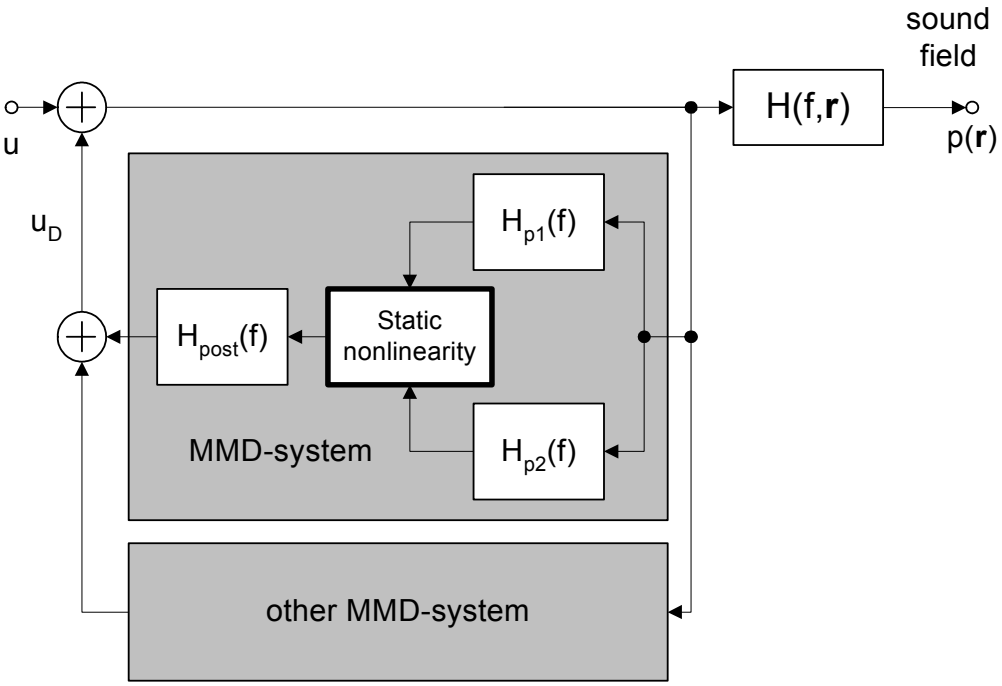

Fig. 11: Modeling of nonlinear mechanism by a MMD systems.

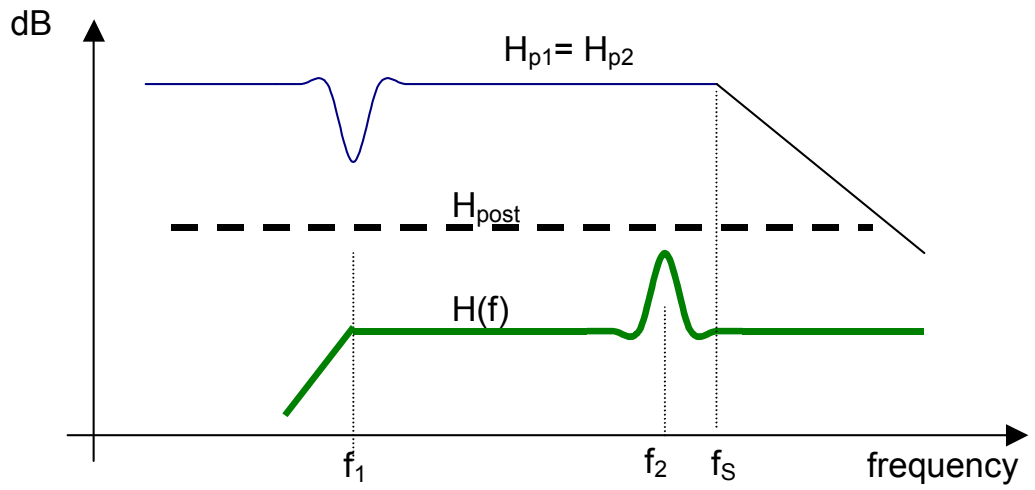

Fig. 12: Amplitude responses (at low frequencies) of the linear pre-system H_{pre} and the linear transfer function *H(f)* of an idealized loudspeaker

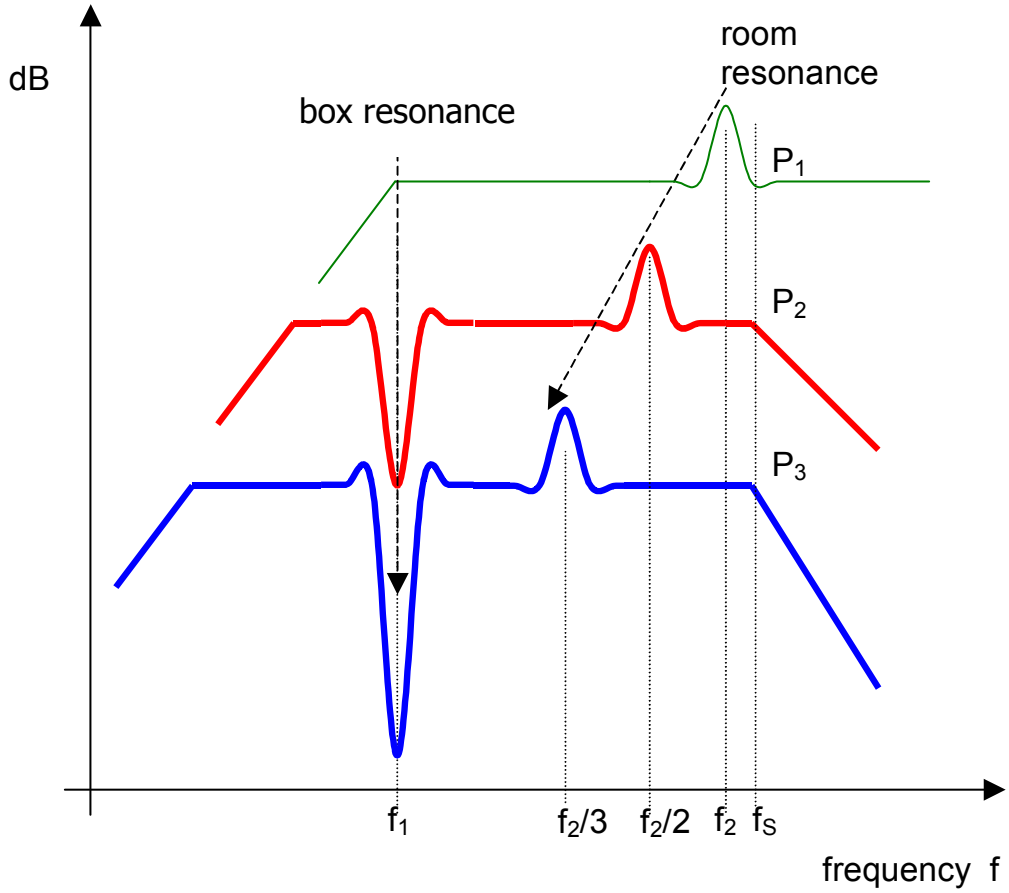

Fig. 13: Amplitude response of the fundamental component P_1, the 2nd-order component P_2 and the 3rd-order component P_3 displayed versus **excitation** frequency f.

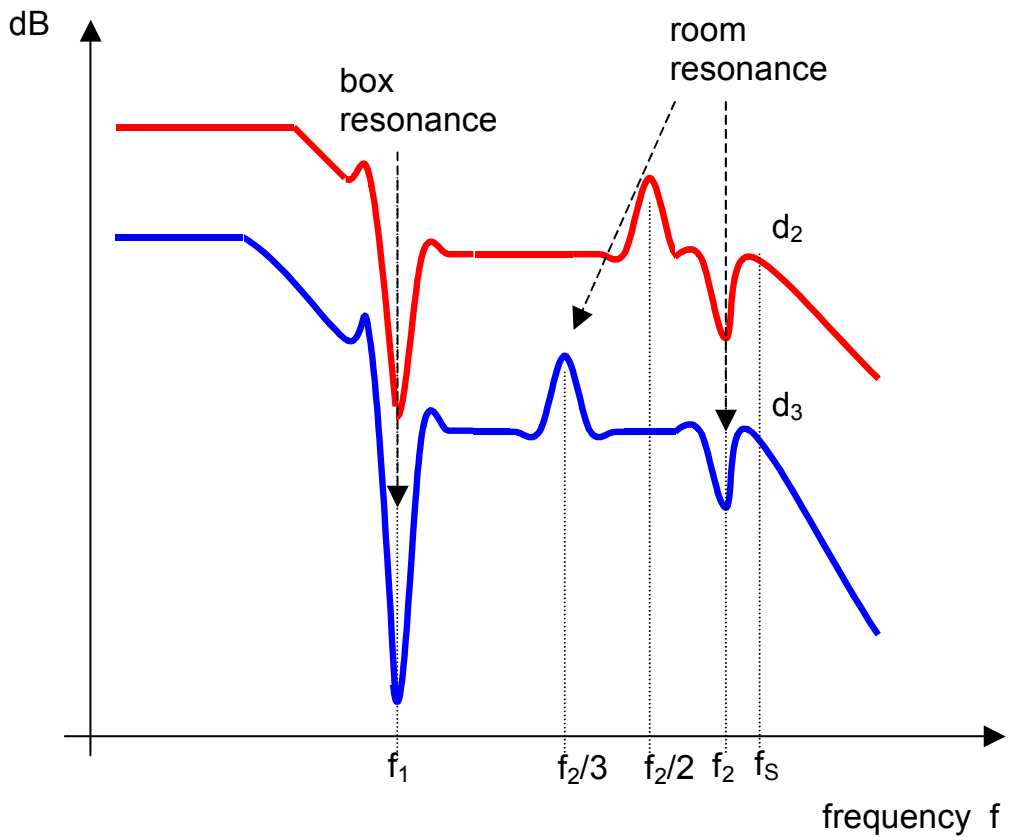

Fig. 14: Amplitude response of 2nd-order distortion d_2 and 3rd-order distortion d_3 in percent displayed versus **excitation** frequency f.

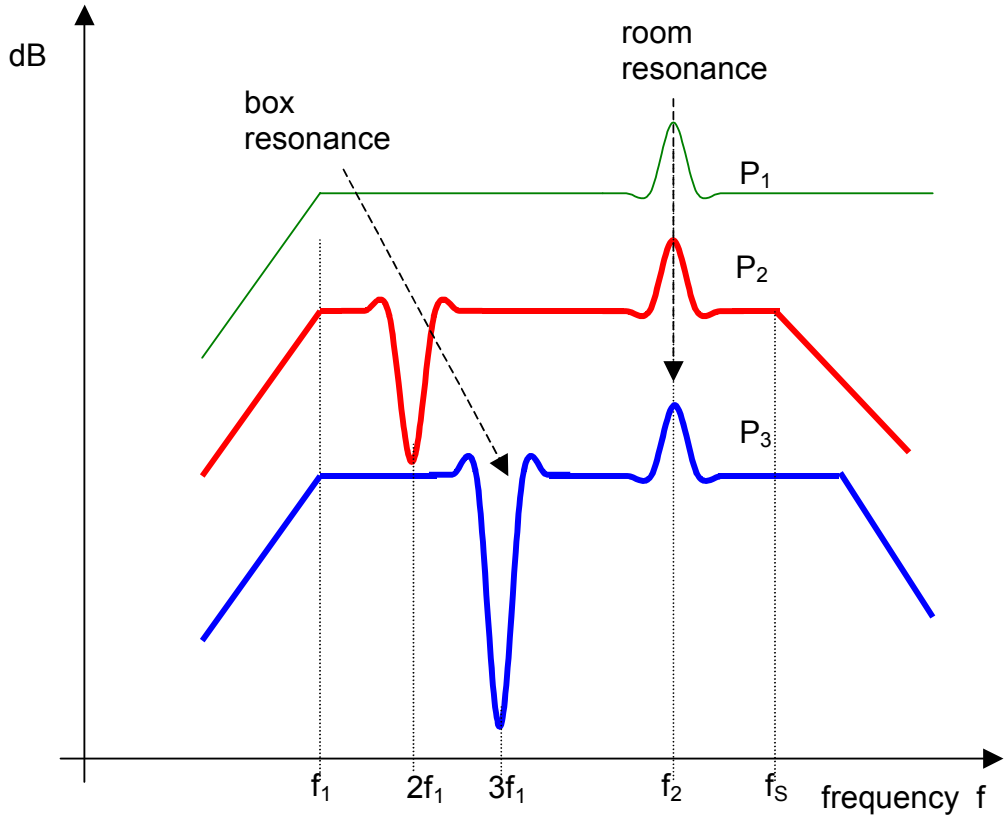

Fig. 15: Amplitude response of the fundamental component P_1, the 2nd-order component P_2 and the 3rd-order component P_3 displayed versus **measured** frequency *f, 2f, 3f,* respectively .

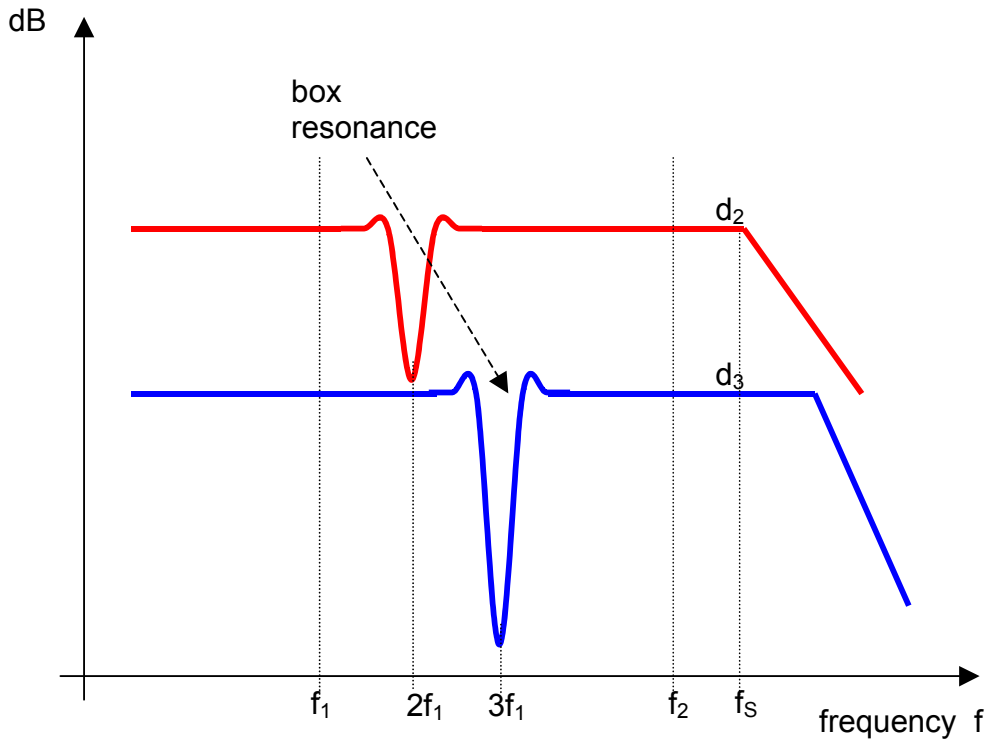

Fig. 16: Amplitude response of 2nd-order distortion d_2 and 3rd-order distortion d_3 in percent displayed versus **measured** frequency *2f, 3f,* respectively .

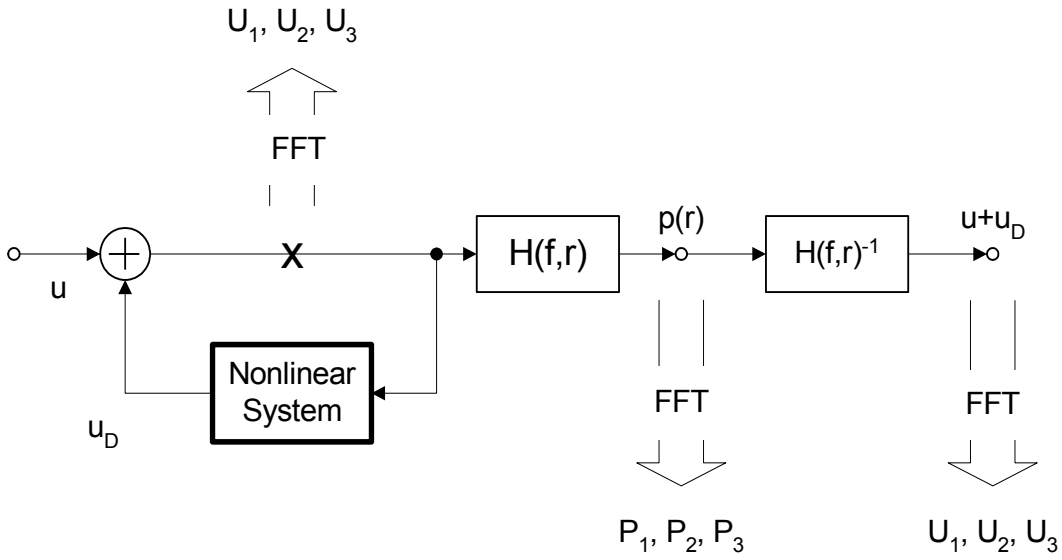

Fig. 17: Measurement of equivalent input distortion by performing a inverse filtering prior to the signal analysis

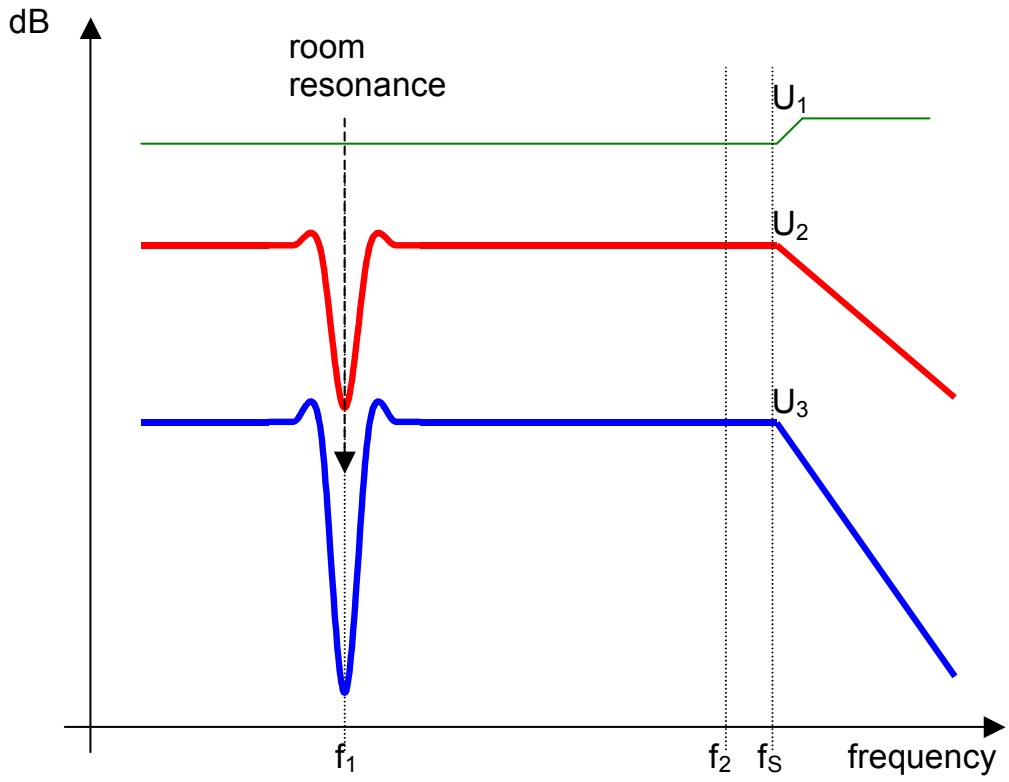

Fig. 18: Fundamental component U_1 and equivalent 2nd-order and 3rd-order harmonic distortion, U_2 and U_3, respectively, mapped to the electrical voltage at the loudspeaker input displayed versus excitation frequency f.

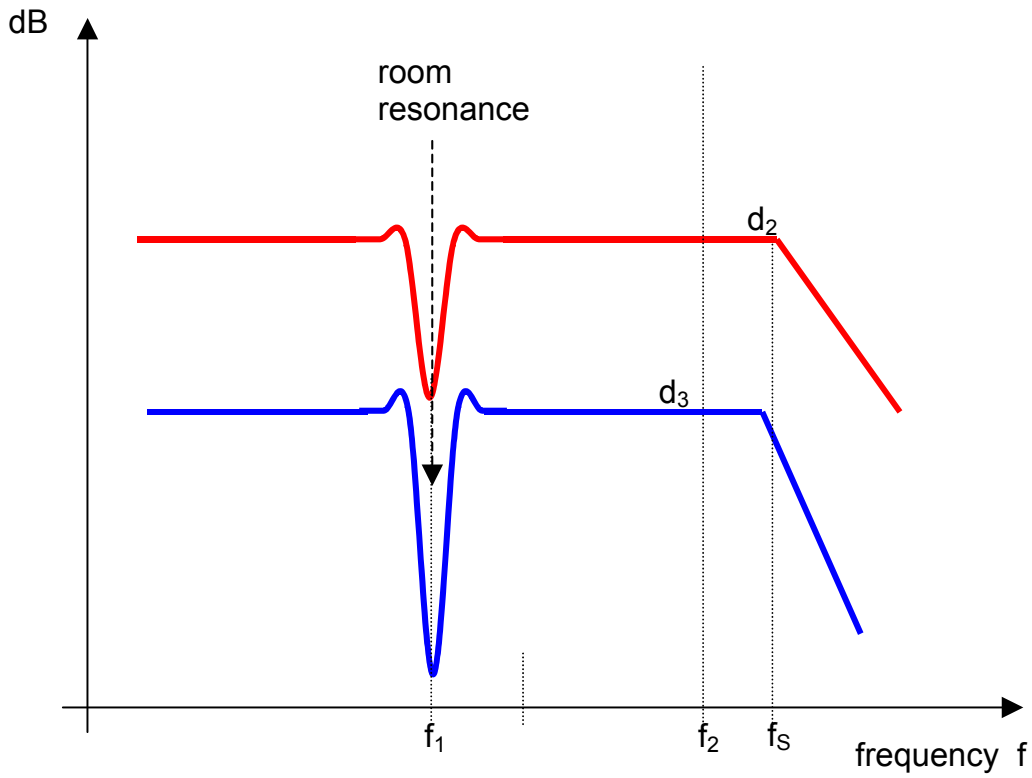

Fig. 19: Amplitude response of 2nd-order distortion d_2 and 3rd-order distortion d_3 in percent displayed versus excitation frequency f .

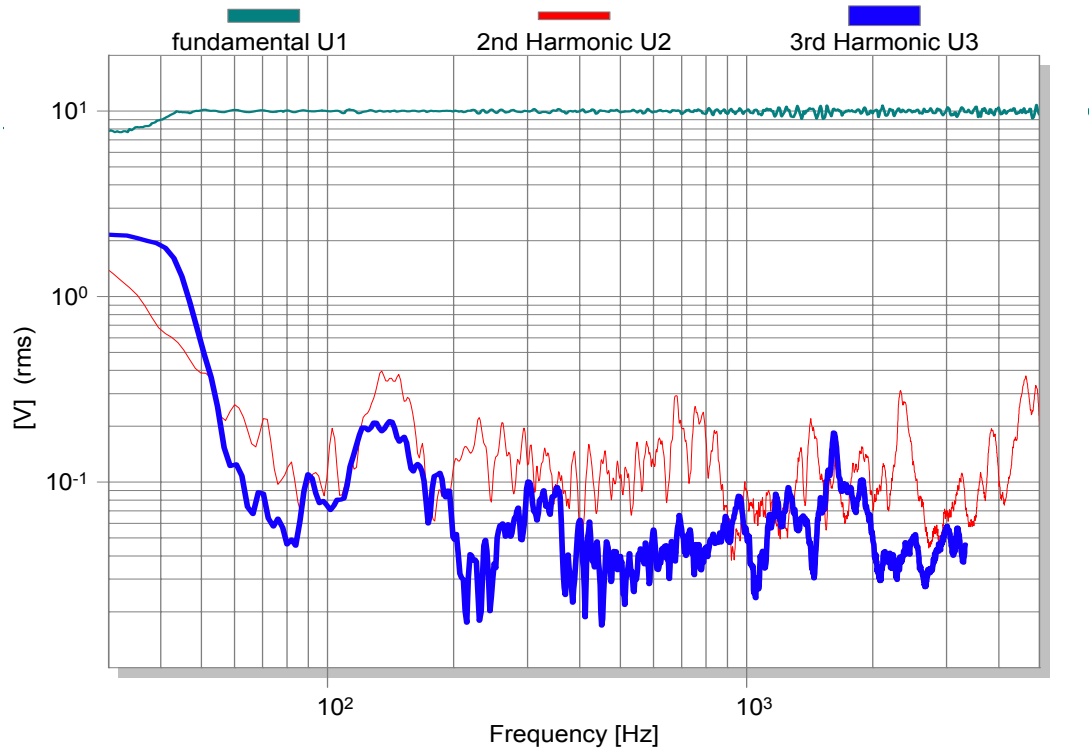

Fig. 20: Equivalent input fundamental U_1 (upper line), 2nd-order equivalent input distortion U_2 (thin line) and 3rd-order equivalent input distortion (thick line) in Volt derived from sound pressure measurement at 1 m distance.

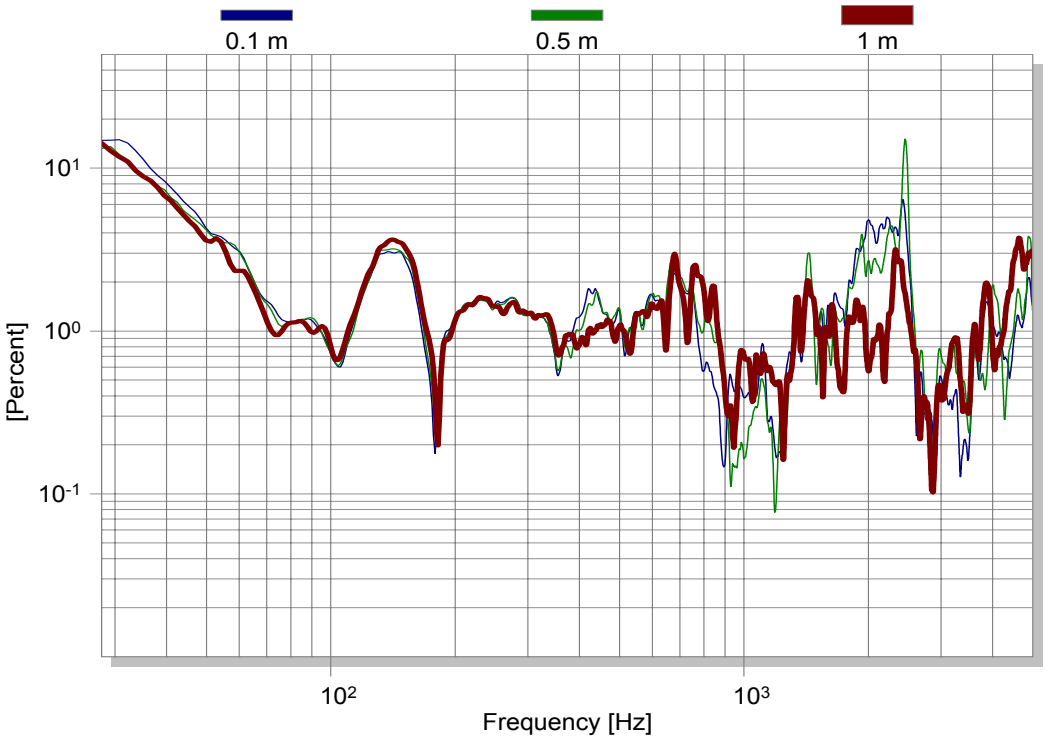

Fig. 21: 2nd-order harmonic distortion equivalent at the input derived from sound pressure measurement at 0.1 m, 0.5 m (thin lines) and 1 m distance (thick line).

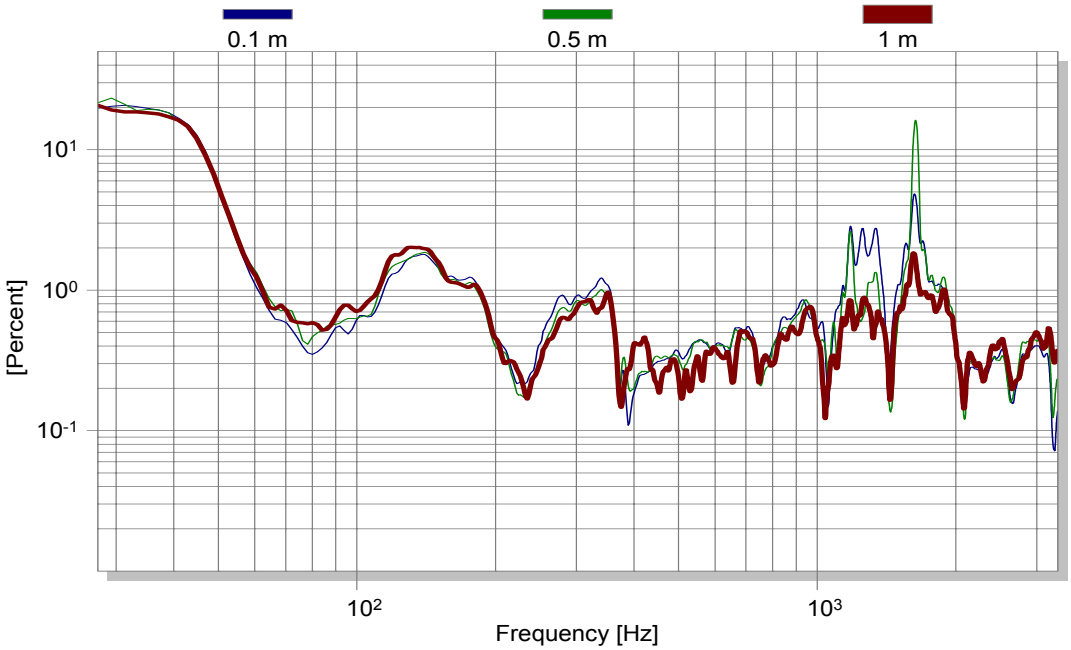

Fig. 22: 3rd-order harmonic distortion equivalent at the input derived from sound pressure measurement at 0.1 m, 0.5 m (thin lines) and 1m distance (thick line).

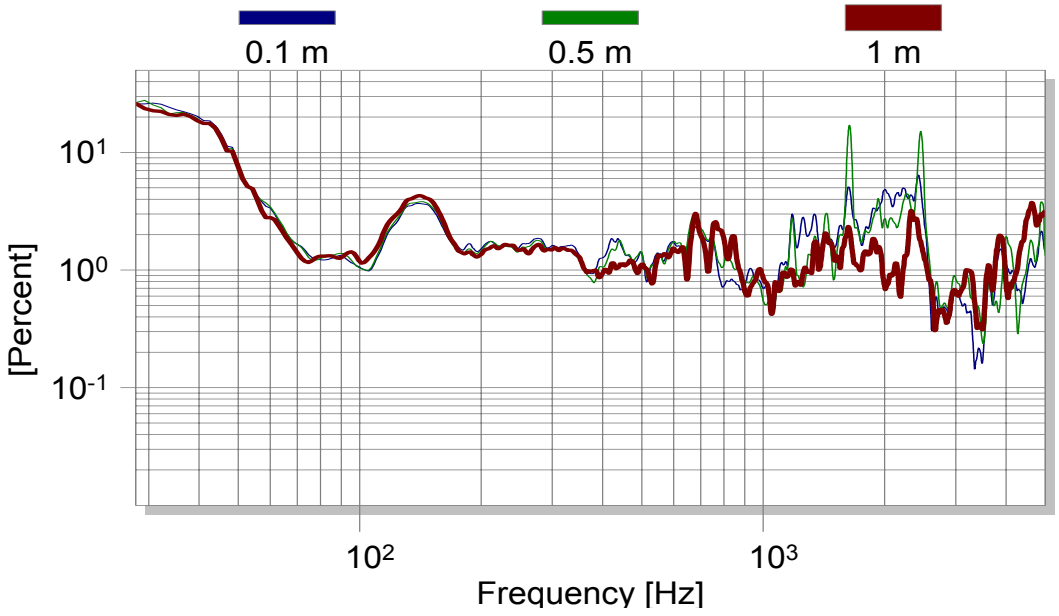

Fig. 23: Total harmonic distortion equivalent at the input derived from sound pressure measurement at 0.1 m, 0.5 m (thin lines) and 1 m distance (thick line).

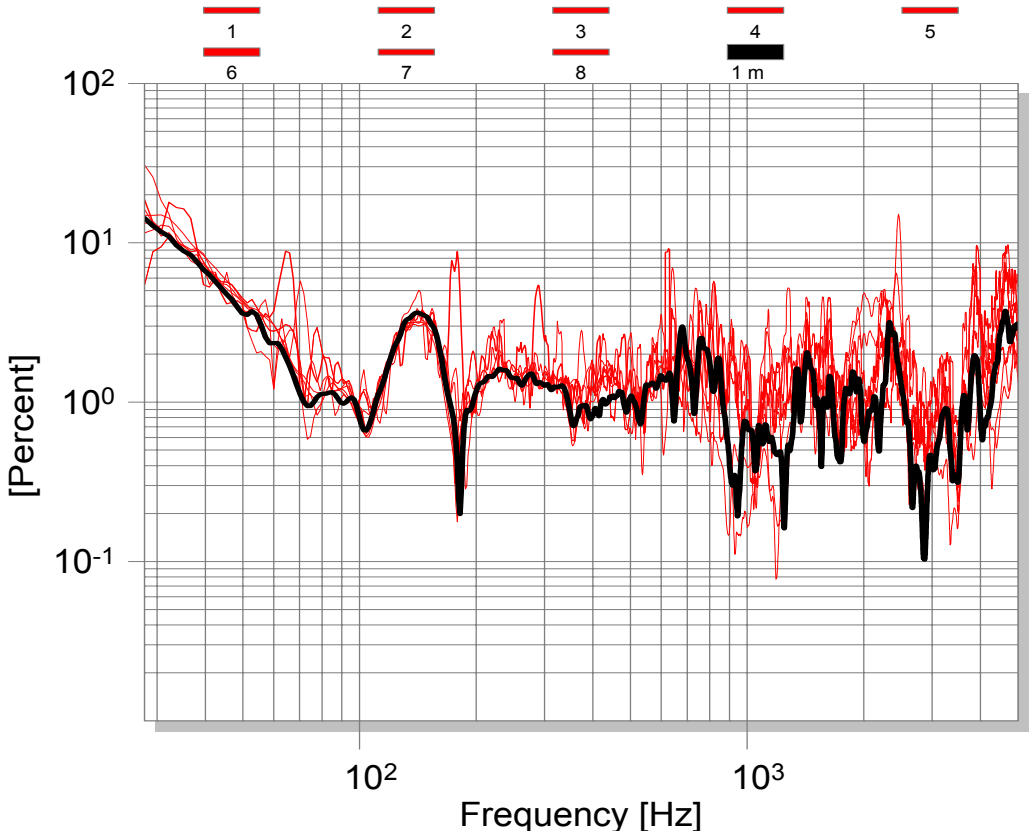

Fig. 24: Equivalent 2nd-order harmonic distortion in percent measured at 1m distance and at 8 different microphone positions in a normal living room.

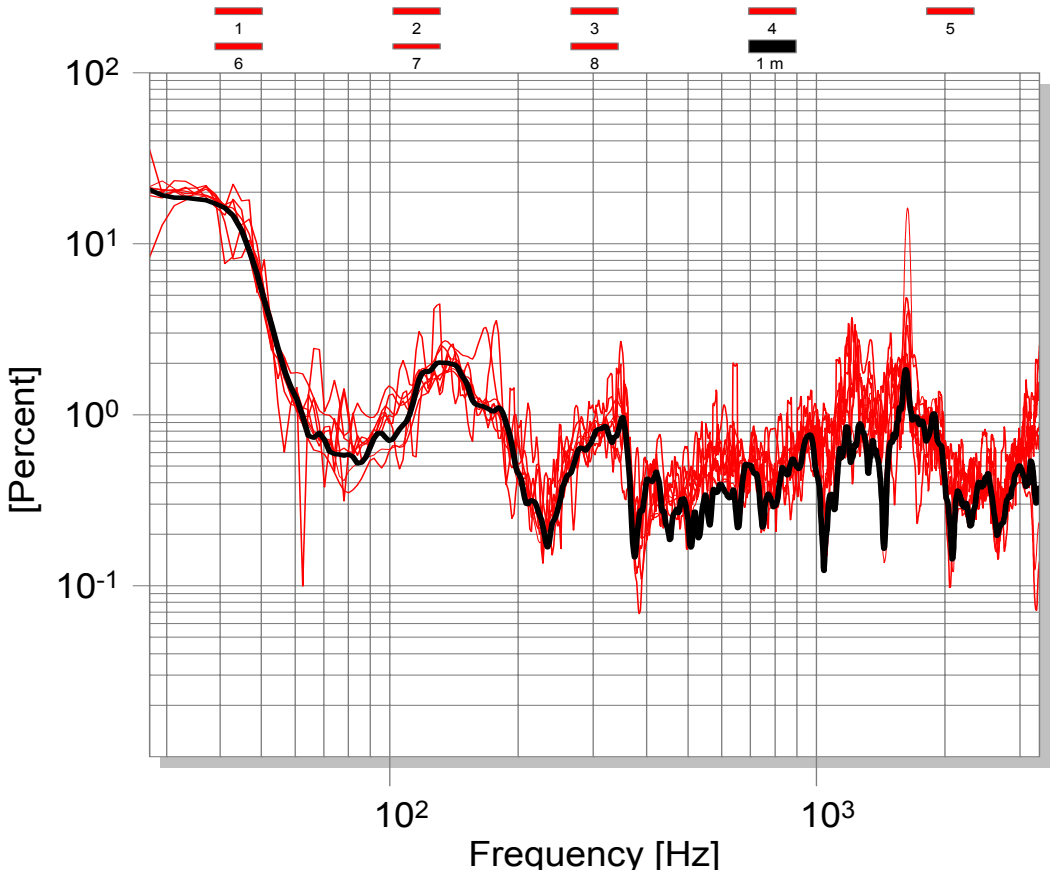

Fig. 25: Equivalent 3rd-order harmonic distortion in percent measured at 1m distance and at 8 different microphone positions in a normal living room.

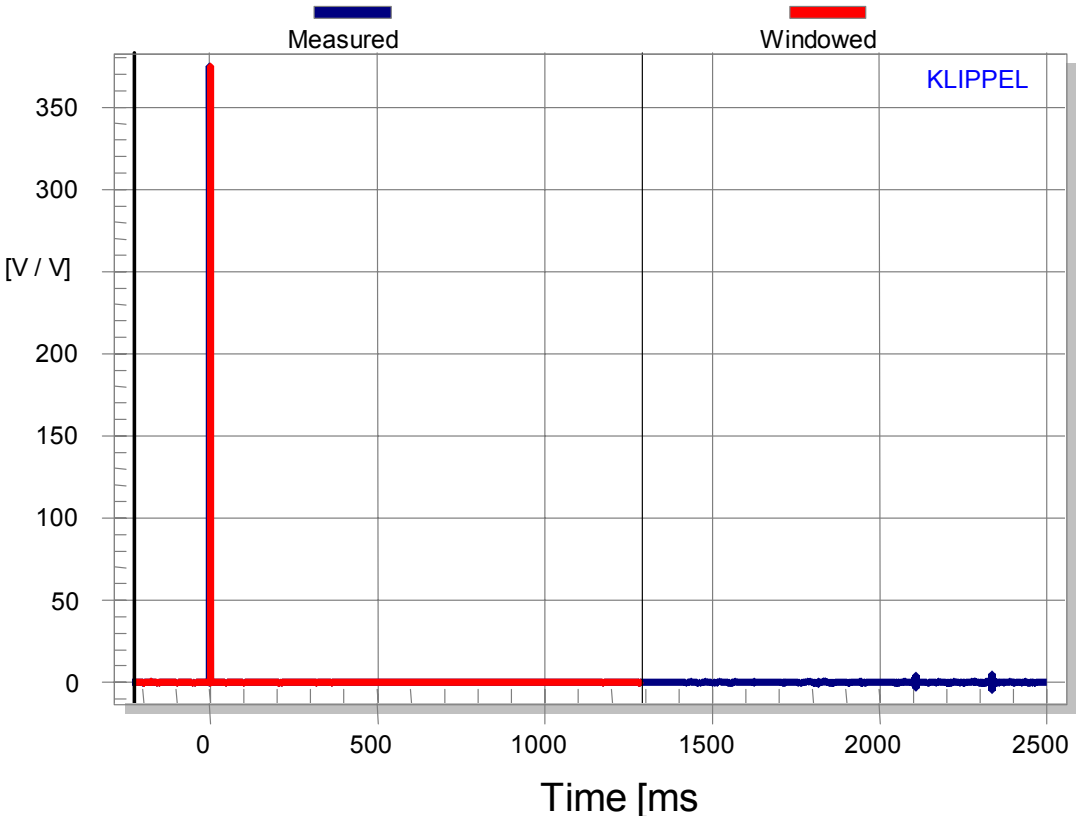

Fig. 26: Time Response of the pre-filtered sound pressure signal.

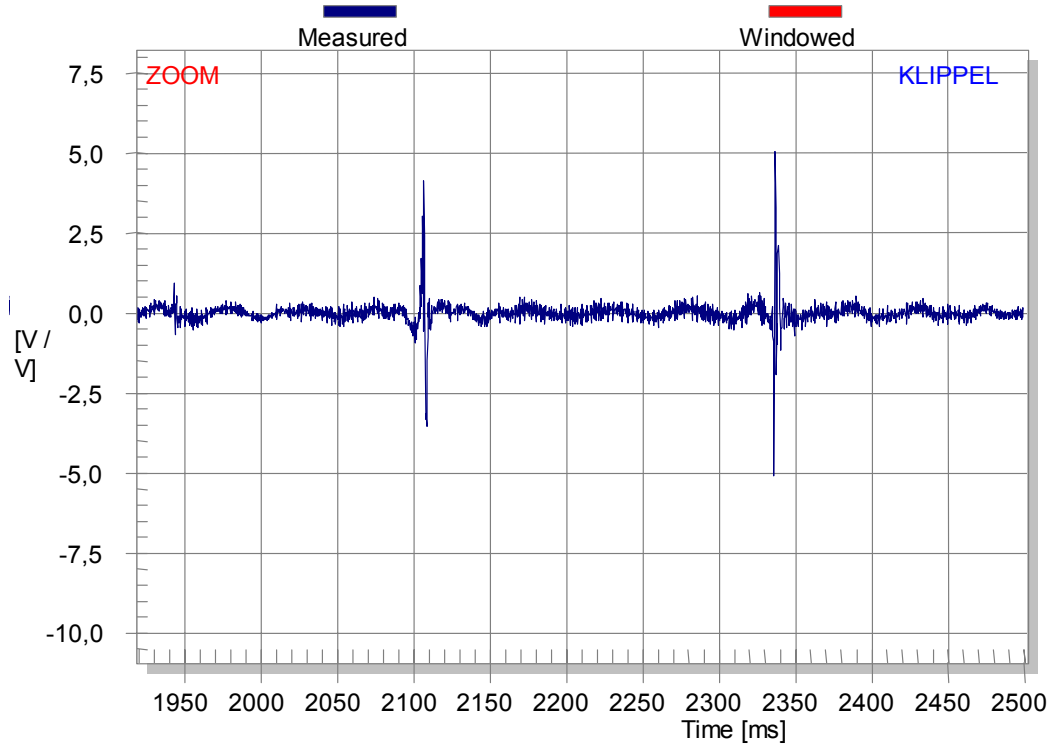

Fig. 27: Detail of the time response in Fig. 26 representing the 2nd-order and 3rd-order equivalent harmonics.

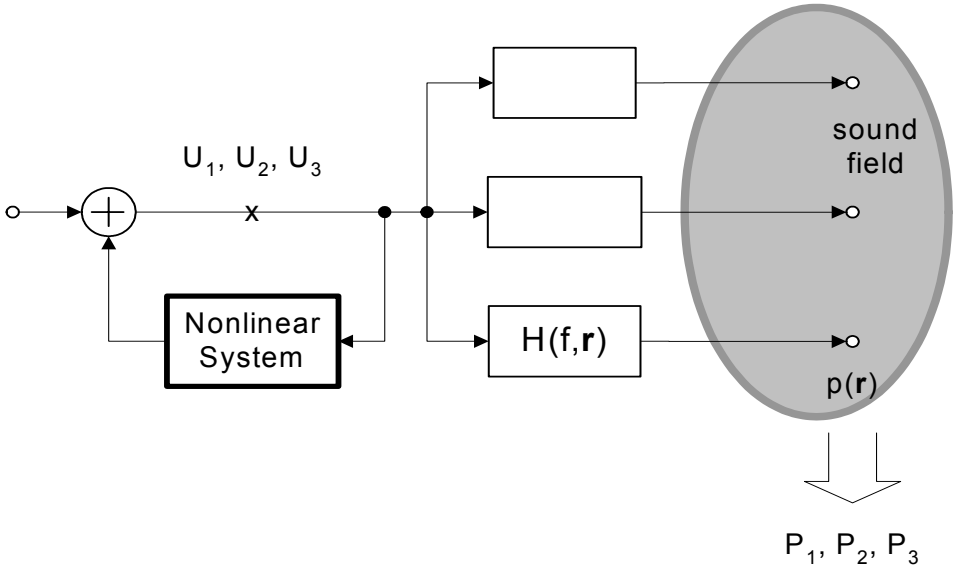

Fig. 28: Prediction of the fundamental and harmonics in the sound pressure output based on equivalent harmonic distortion filtered with the linear transfer function $H(f,\mathbf{r})$.

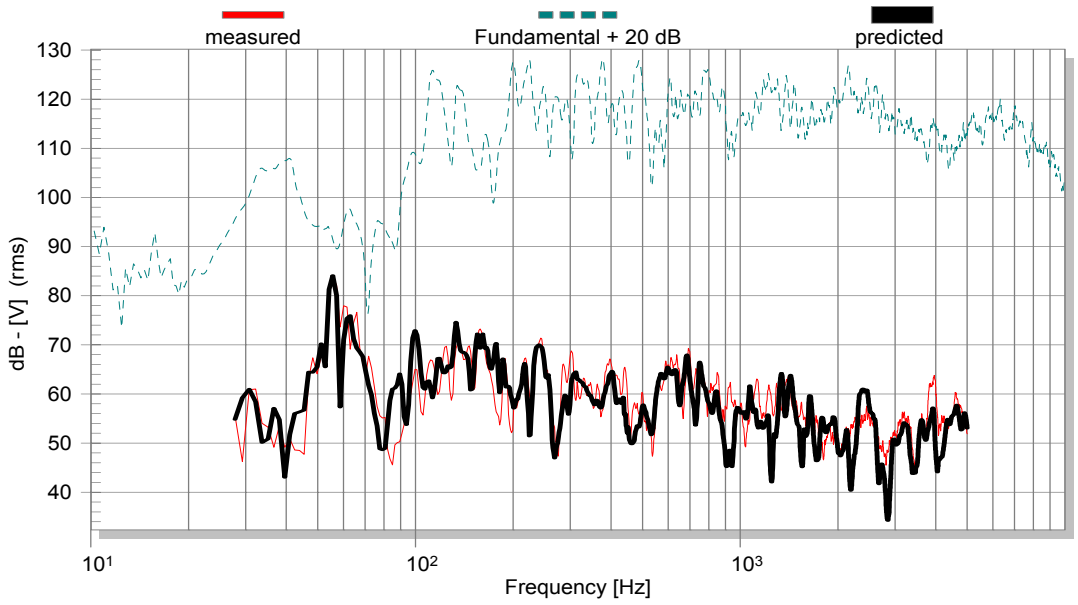

Fig. 29: Fundamental response P_1 and 2^{nd}-order harmonic distortion component P_2 measured and predicted at point $\mathbf{r}_7$ in the room.

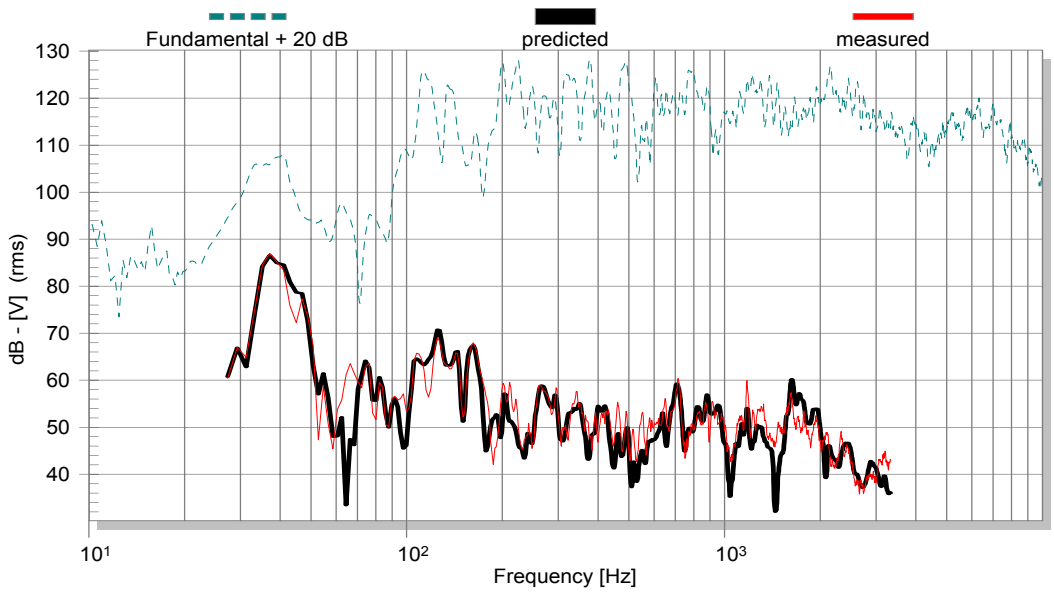

Fig. 30: Fundamental response P_1 and 3rd-order harmonic distortion component P_3 measured and predicted at point $\mathbf{r}_7$ in the room.

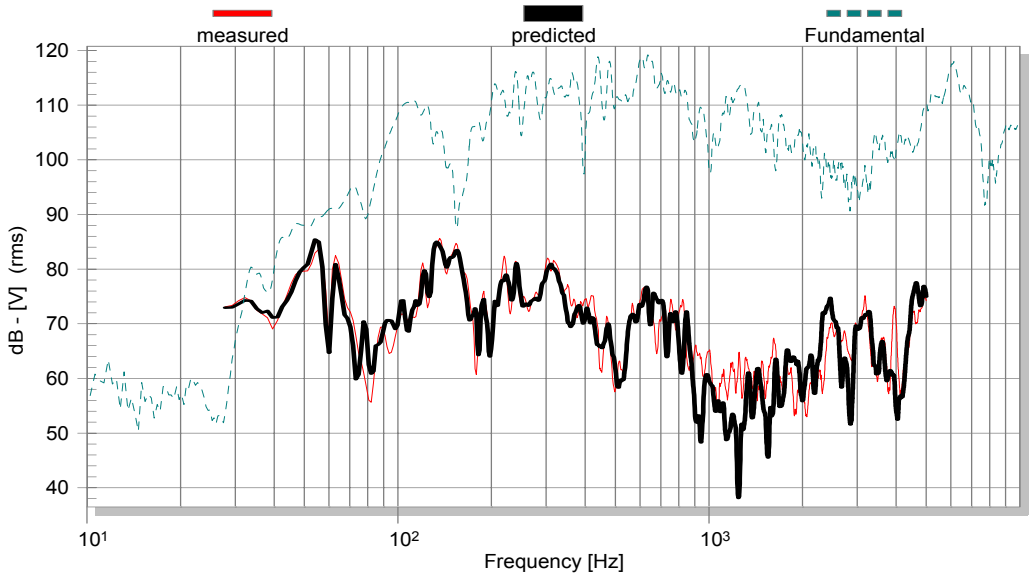

Fig. 31: Fundamental response P_1 and 2nd-order harmonic distortion component P_2 measured and predicted at point $\mathbf{r}_5$ in the room.

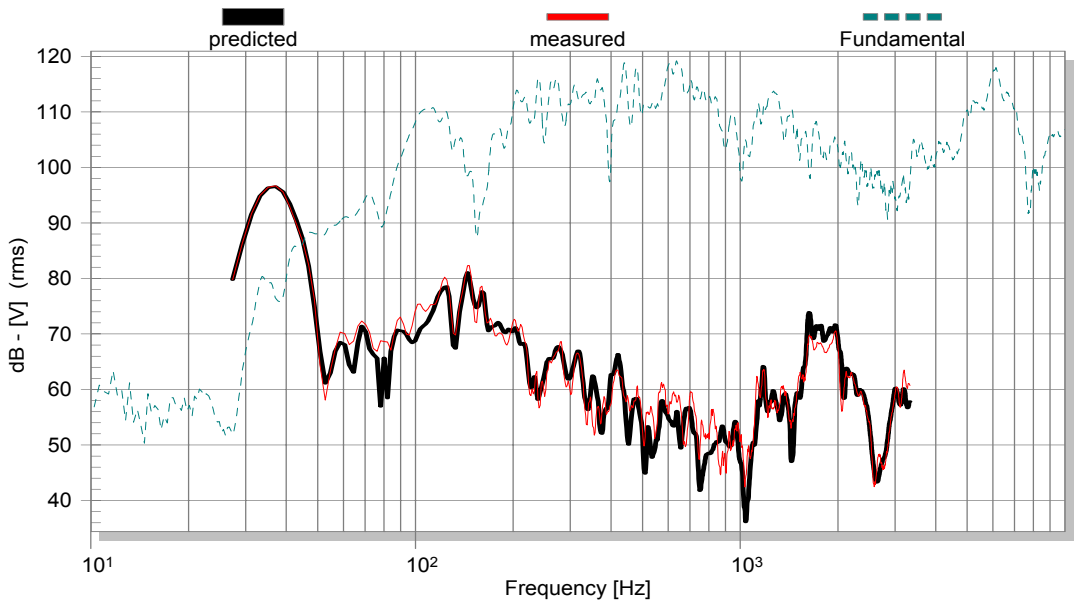

Fig. 32: Fundamental response P_1 and 3rd-order harmonic distortion component P_3 measured and predicted at point $\mathbf{r}_5$ in the room.

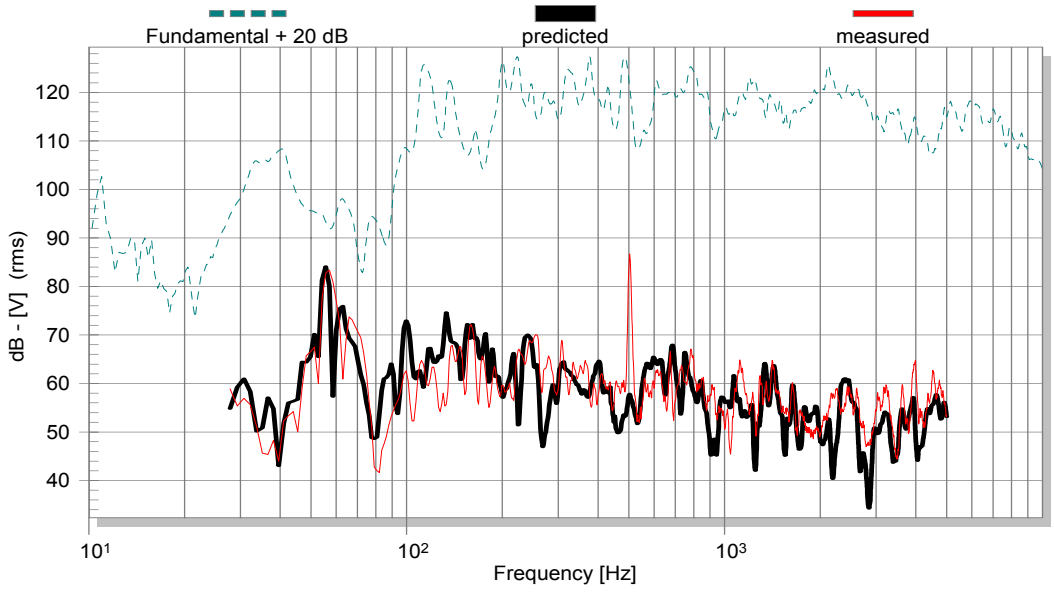

Fig. 33: Detection of a stationary disturbance (1 kHz tone) in the 2nd-order harmonic distortion component by comparing the predicted and measured distortion.

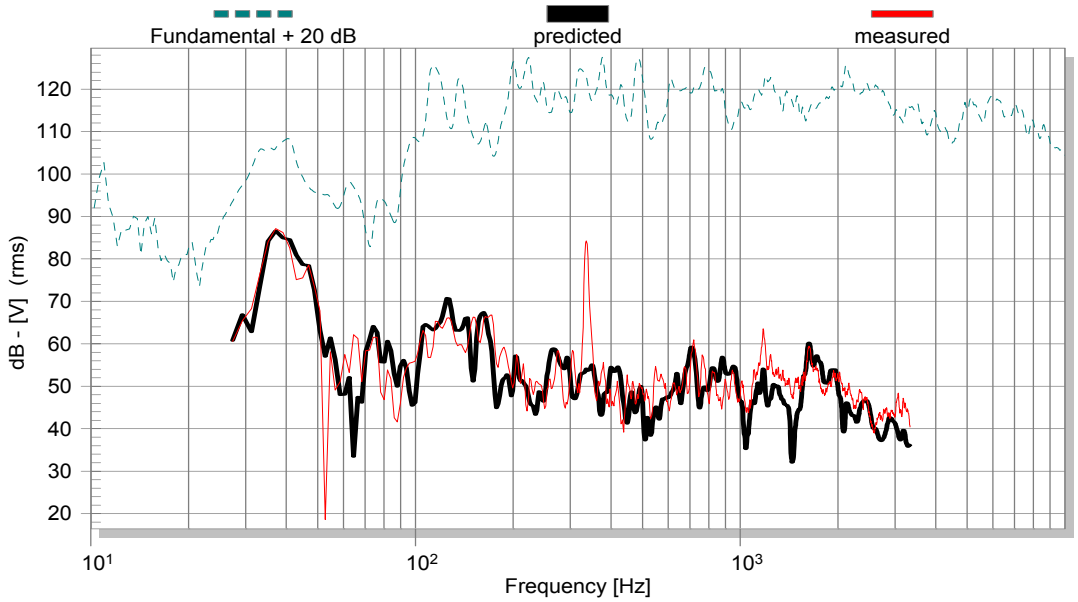

Fig. 34: Detection of a stationary disturbances (1 kHz tone) in the 3rd-order harmonic distortion component by comparing the predicted and measured distortion.

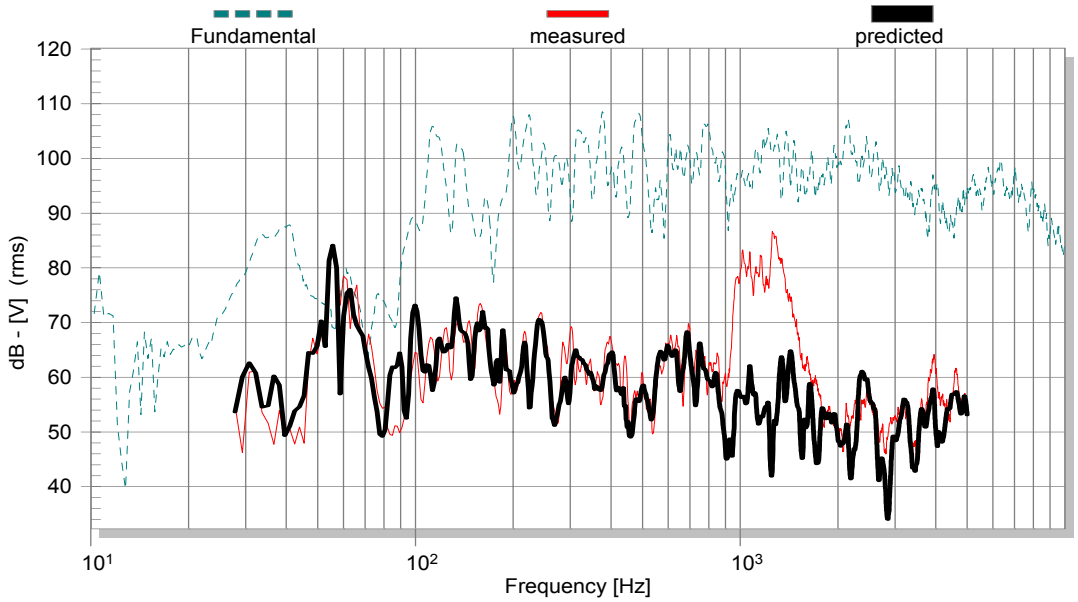

Fig. 35: Separation of a transient disturbance (shutting the door) by comparing the predicted and measured 2nd-order harmonic distortion component P_2.

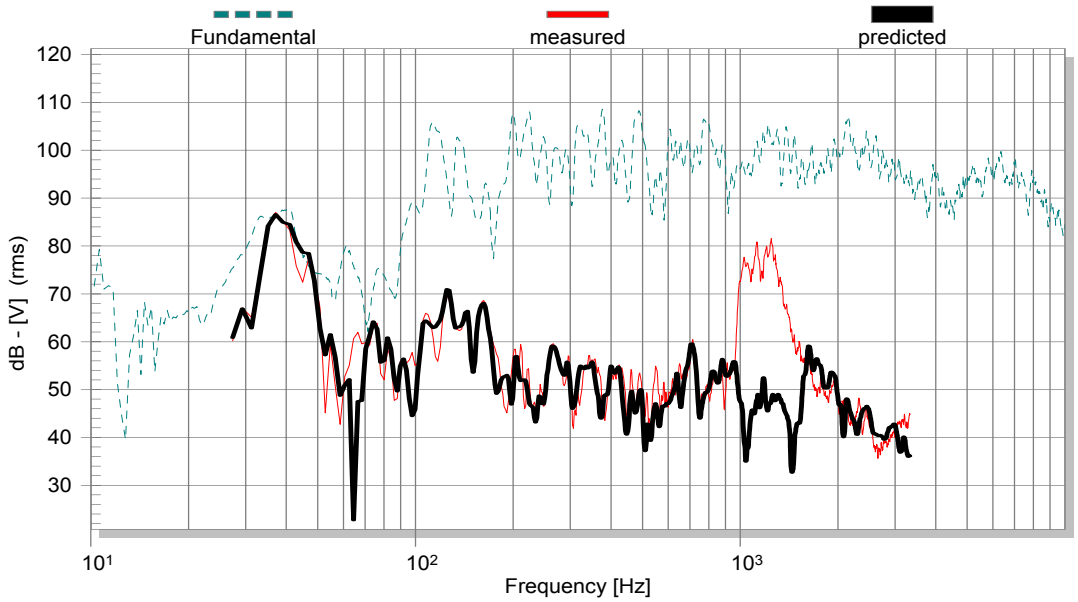

Fig. 36: Separation of a transient disturbance (shutting the door) by comparing the predicted and measured 2nd-order harmonic distortion component P_2.

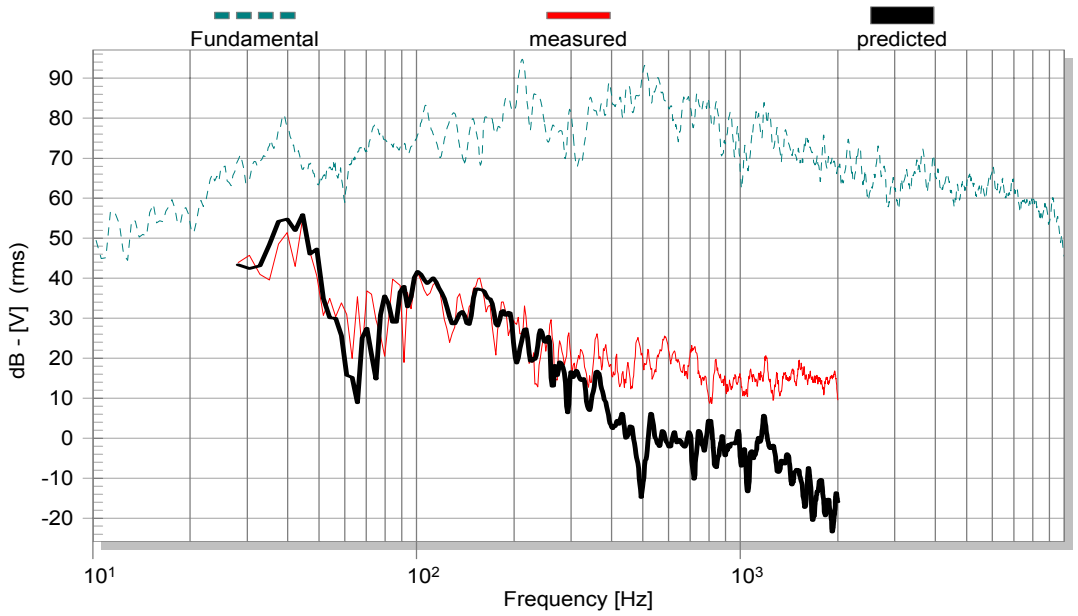

Fig. 37: Detection of a disturbances (noise) in the 5th- harmonic distortion component by comparing the predicted (thick line) and measured (thin line) distortion.

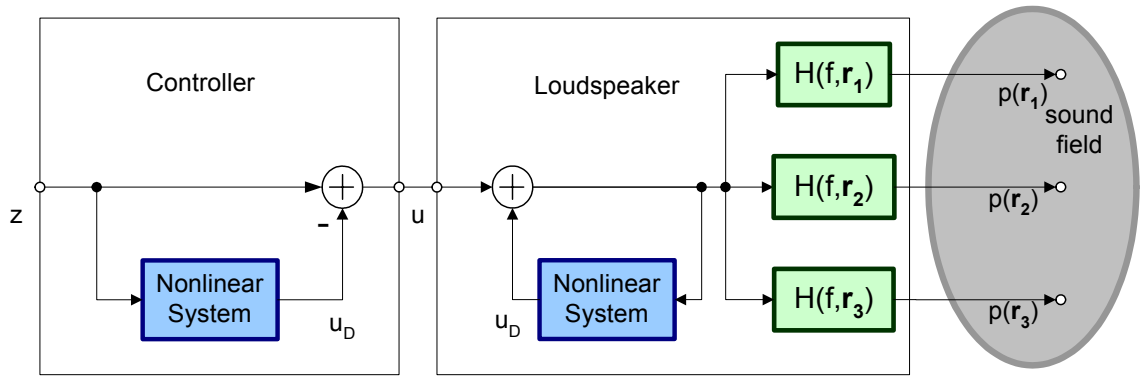

Fig. 38: Active Compensation of Equivalent Input Distortion by Nonlinear Control.

TABLES:

Mechanism	**Static Nonlinearity**	**Multiplied Signals**	**$H_{p1}(f)$**	**$H_{p2}(f)$**	**$H_{post}(f)$**
suspension	$K_{ms}(x)x$	displacement x	low-pass	low-pass	=const.
motor force	$Bl(x)i$	displacement x, current i	notch-filter	low-pass	=const.
electrical damping	$v/Bl(x)^2$	displacement x, velocity v	band-pass	low-pass	=const.
inductance	$L_e(x)i$	displacement x, current i	notch filter	low-pass	differentiator

Table 1: Properties of the linear systems and the static nonlinearity